LONG-TERM VARIABILITY IN OFFSHORE WIND SPEEDS

by

Ag Stephens

Thesis presented in part-fulfilment of the degree of Master of Science in accordance with the regulations of the University of East Anglia

School of Environmental Sciences
University of East Anglia
University Plain
Norwich
NR4 7TJ

July 2000

ABSTRACT

The growth of interest in offshore wind power has led to the need for accurate long-term wind speed estimates for the siting of wind turbines. A comprehensive dataset is lacking due to inconsistent measurement techniques. A standardised predictive method has been sought and the most promising approach involves use of surface pressure data and the geostrophic wind.

A historical dataset of mean sea level pressure values is used here to derive offshore wind speeds over European waters from 1881-1995. The data is compared with Reanalysis modelled wind speeds for the last 50 years. The correlation between the two datasets is relatively high, particularly over the open ocean and in winter. Anomalies in the derived data are corrected using trends in the Reanalysis winds. The region to the north-west of the UK exhibits the highest long-term wind speeds and the highest variability.

Significant correlation is found between both datasets and the North Atlantic Oscillation in the North Atlantic, North Sea and Baltic Sea. Decadal mean wind speeds are calculated at a number of grid points. These are used to estimate variation in energy production from offshore wind turbines. Corrected mean wind speeds are shown to vary from decade to decade by up to 0.9 metres per second, significantly affecting the potential power generation from a wind turbine.

CONTENTS

Page Number

ABSTRACT

CONTENTS

List of Figures
List of Tables

1. INTRODUCTION

1.1 Context
1.2 Offshore Wind Energy and the European Union
1.3 The Offshore Wind Resource
    1.3.1 Offshore Wind Speed Measurements
    1.3.2 Models to Predict Offshore Wind Speeds
    1.3.3 The Predicting Offshore Wind Energy Resource (POWER) Project
1.4 Long-term Variability in Wind Speeds
1.5 The North Atlantic Oscillation
1.6 Summary
1.7 Hypothesis, Aims and Objectives

2. METHODS AND DATA

2.1 Methods to Calculate Wind Speeds
    2.1.1 Geostrophic Wind Speeds
    2.1.2 Pressure Gradients
    2.1.3 Surface Wind Speeds
    2.1.4 Wind Turbine Hub Heights
    2.1.5 Wind Direction
    2.1.6 Assumptions and Simplifications of the Model
2.2 Datasets
    2.2.1 UKMO Daily Mean Sea Level Pressure (MSLP)
    2.2.2 NCEP/NCAR Monthly Mean 10 m Wind Speeds
    2.2.3 Data Acquisition
2.3 Data Transformation
    2.3.1 Interpolation of the Daily Pressure Grid
    2.3.2 NCEP/NCAR Wind Speeds
    2.3.3 UKMO MSLP
    2.3.4 Modifying the Interpolation Method
    2.3.5 Checking the Interpolated MSLP
2.4 Statistical Methods
    2.4.1 Linear Regression and Comparison of Means
    2.4.2 Low-pass Filtering

3. RESULTS

3.1 Adjustment of the Start Year to 1883
3.2 Comparisons of the Model Output with Wind Speeds Measurements
3.3 Comparing Derived and NCEP/NCAR Wind Speeds
    3.3.1 General Trends
    3.3.2 Comparison of Means and Correlations
    3.3.3 Interannual Variability
3.4 Correlations Between Wind Speeds and the NAO
3.5 Time Series Analysis
3.6 Correcting Errors in the UKMO MSLP Dataset
    3.6.1 The 1960-65 period
    3.6.2 The 1899-39 period

4. DISCUSSION

4.1 Validity of the Method
4.2 Derived and NCEP/NCAR Wind Speeds
4.3 Long-term Trends
4.4 Spatial Correlation Between Grid Points
4.5 Relating the NAO To Surface Winds
4.6 Long-term Variability
4.7 Relating Mean Wind Speeds to Power Output and Economic Implications for Offshore Wind Energy

5. CONCLUSIONS

5.1 Long-term Variability in Offshore Wind Speeds
5.2 Suggestions for Further Work

REFERENCES

ACKNOWLEDGEMENTS

APPENDIX 1: List of Abbreviations

APPENDIX 2: Fortran 77 Programme to read the MSLP grid and calculate wind speeds

APPENDIX 3: Anomalies Identified in the UKMO MSLP Dataset

APPENDIX 4: The seasonal pattern in wind speeds

LIST OF FIGURES

Figure **Page**

1. A schematic of the POWER methodology [Source: Watson *et al*, 1999].

2. The winter NAO index (Dec-March) from 1821-1999 [Data source: CRU, 2000].

3. Original and post-interpolated NCEP/NCAR monthly wind speeds for January 1948 over the UK.

4. Annual long-term means for derived and NCEP/NCAR datasets from 1948-95.

5. Monthly standard deviations for derived and NCEP/NCAR datasets showing the seasonal and interannual variability from 1948-95.

6. Annual standard deviations for derived and NCEP/NCAR datasets showing the interannual variability.

7. The locations of grid points 1-16.

8. Mean monthly R^2 values correlating NCEP and derived data averaged across 16 grid points from 1948-95.

9. A contour plot of the correlation between the monthly mean NCEP/NCAR and derived wind speeds.

10. A bar chart showing R^2 values for the correlation of derived and NCEP/NCAR datasets with the NAO index.

11. A 21-year running correlation between the NAO index and mean winter 10 m wind speeds at grid point 9.

12. Time series plots showing derived and NCEP/NCAR 10 m wind speeds at grid points 1 and 12.

13. Annual mean 80 m wind speeds at grid points 2, 5, 12 and 14.

14. Lower 95% confidence limits for mean annual 80 m wind speeds.

15. Estimated decadal mean energy production from a wind turbine at grid point 12 from 1886-1995.

16. Monthly averages at grid points 3 and 12 in the derived and NCEP/NCAR data.

17. The location of grid point 2 and comparative sites.

LIST OF TABLES

Table **Page**

1. A comparison of curves to describe the relationship between friction velocity and geostrophic wind speed.

2. NCEP/NCAR Reanalysis data sources [Source: Kalnay *et al*, 1996].

3. Observed and modelled mean wind speeds at 20 m height (ms^{-1}).

4. Summary statistics and difference in means for the derived and NCEP/NCAR monthly mean 10 m wind speeds at grid points 1-16.

5. Observation times for each time period in the UKMO dataset [Source: Jones, 1987].

6. Correlations between the NCEP/NCAR and derived annual wind speeds at grid points 1-16.

7. Correlation matrix showing R^2 values between decadal mean wind speeds at grid points 1-16.

1. INTRODUCTION

The topic of wind energy generation related to offshore wind speeds is introduced. The literature suggests that a comprehensive dataset is lacking, methods of predicting offshore wind speeds are discussed. Long-term variability of wind speeds and the North Atlantic Oscillation are introduced. The hypothesis, aim and objectives are stated.

1.1 CONTEXT

Threats to human health, ecosystems and the global climate, due to the combustion of fossil fuels, have led to increased interest in alternative sources of energy. The government has set a target to provide 10% of the UK's electricity from renewable energy by 2010 (DETR, 1998). Wind power is one of the most promising renewable energy sources in the UK. However, due to problems in obtaining planning permission and local objections to onshore projects, greater emphasis has recently been placed on offshore locations (Palutikof *et al*, 1997). At present little is known about the extent of the offshore resource because reliable wind speed data is scarce (Barthelmie *et al*, 1991). Observational and measuring techniques vary greatly with the result that a comprehensive dataset in European waters is lacking, in both space and time (Watson *et al*, 1999).

Knowledge of spatial variation is required to identify the best locations for siting wind farms. Temporal variation (from interdecadal to diurnal) should also be examined in order to predict the economic viability of a wind farm and to assess the energy output for turbines attached to the national grid (Watson *et al*, 1999).

The North Atlantic Oscillation (NAO) has been shown to exhibit interannual and interdecadal variability that has been related to climatic variations over Europe (Mehta *et al*, 2000) and to greenhouse-gas induced regional climate change (Paeth *et al*, 1999). Wind speeds over Europe may show a variability related to that of the NAO. This work involves the creation and analysis of a long-term wind speed dataset to examine variability on the interannual and interdecadal scales.

1.2 OFFSHORE WIND ENERGY AND THE EUROPEAN UNION

Renewable sources account for 13.9% of electricity* generated in the European Union (EU) and targets have been set for 22% to be supplied by 2010 (ENDS, 2000).

* The figures quoted are for electricity generation and not total energy use. The European Commission is currently in the process of drafting a directive that will create a 2010 target of 12% of gross energy consumption from renewable sources (ENDS, 2000).

The UK generates only 1.7% of its electricity from renewable sources at present, this will have to rise to 10% in the next 10 years to reach the current Government target.

The UK has a significant offshore wind resource estimated at 986 TWh yr^{-1} in a study of offshore wind in the European Community (Matthies *et al*, 1994). This is almost three times the total annual UK electricity use in 1996 (344 TWh (Stationary Office, 1997)) and is just under a third of the total EU offshore resource. This plentiful resource is currently untapped. The first UK offshore wind farm is under construction at Blyth where two 750 kW turbines will be installed by September 2000 (Border Wind, 1998). The speed with which the industry can be advanced will have a major effect on whether the UK reaches its 10% target.

1.3 THE OFFSHORE WIND RESOURCE

1.3.1 OFFSHORE WIND SPEED MEASUREMENTS

There is a lack of consistent meteorological data from offshore areas. Wind speed is a geophysical variable that requires very accurate measurement because there is generally a small signal-to-noise ratio and there is high short-term variability (Stoffelen, 1998). Traditionally, measurements of offshore wind speed have been obtained from such varied sources as meteorological stations, oil and gas platforms, buoys and a range of different ocean going vessels (Wu, 1995). These methods generally rely on the use of anemometers to measure the wind. There is much variation in the methods employed and therefore the dataset is inhomogeneous and questionable (Barthelmie, 1993). More recently, methods have included numerical weather prediction models and satellite measurements (Wu, 1995).

Barthelmie (1993) reviews methods of measuring offshore wind speeds. Each method has its own advantages and disadvantages, ranging from flow distortion (due to structures blocking the wind) to problems with sampling time. Estimates of wind speeds by observation of the sea surface depend on the skills and judgement of individuals. Significant errors can occur with both estimation and measurements of ocean winds. Other factors such as varied measuring heights and averaging times prevent adequate inter-calibration of the datasets (Barthelmie, 1993).

Techniques have also been developed to measure sea surface winds using remote sensing (Kidder & Vonder Haar, 1995), but all rely on calibration with surface data. Satellite data is ‘tuned’ using buoy and ship measurements of wind speed (Wu, 1995).

The best method of examining the offshore wind field involves performing wind speed measurements at a proposed site over a long period of time. However, this is very expensive so indirect methods have been developed to predict offshore wind speeds. A discussion of these techniques follows.

1.3.2 MODELS TO PREDICT OFFSHORE WIND SPEEDS

The prediction of offshore winds is considered simpler than predicting land based wind speeds due to the flattened topography of the ocean (Barthelmie, 1993). Some studies have suggested a simple relationship to explain the change in wind speed from land to ocean. For example, Hsu (1988) suggests that the sea surface wind (U_{SEA}) can be related to the coastal wind (U_{LAND}) by the equation:

$$U_{SEA} = 1.62 + 1.17\, U_{LAND} \qquad \text{(Eq. 1.1)}$$

This simplified method does not incorporate important factors such as roughness, topography and fetch. White (1985) uses a similar technique but includes the effects of roughness around each site, and extends the dataset to a 1° grid square over the ocean.

Troen and Petersen (1989) developed the European Wind Atlas based on data from European meteorological stations. Observations are corrected for local effects to take account of topography, sheltering and roughness. The drawback with this technique is the dependence on land-based stations for predicting ocean winds.

Moore (1982) developed the 900 mb model based on upper air wind speeds from radiosonde data at nine UK sites. Barthelmie (1991) revised the model, generating an upper air wind field on a 10 km grid square, used to calculate near surface winds.

Børresen (1987) uses Mean Sea Level Pressure (MSLP) data to calculate the geostrophic wind. This is transformed to a mean wind speed at 10 m above sea level. Estimated wind speeds are validated by ship and lighthouse measurements. Børresen's geostrophic wind method has shown good agreement with Barthelmie's adjusted 900 mb model. Both these models have performed well, predicting wind speeds within 0.5 ms^{-1} of observed values at sites of most reliable data quality (Barthelmie, 1993).

Barthelmie (1997) has also examined methods of predicting winds across the land-sea interface, showing that no model performs well at all hub heights. The need for any offshore prediction method to involve wind speed corrections around the coastal discontinuity is demonstrated.

A comparison of methods used to predict offshore winds suggests that the geostrophic or upper air flow model is most likely to be suitable in future work. Such a method has recently been adopted by the POWER (Predicting Offshore Wind Energy Resources) project, funded by the European Commission (Watson *et al*, 1999).

1.3.3 THE PREDICTING OFFSHORE WIND ENERGY RESOURCE (POWER) PROJECT

The three-year POWER project* (set up in August 1998) aims to develop a methodology for predicting long-term wind resources which do not rely directly on offshore anemometer data. It will be used to identify the best sites available for wind farm operation in European waters (Watson *et al*, 1999). Detailed monitoring at identified locations will then be used to validate the method and refine the estimates. Figure 1 shows a schematic of the POWER methodology.

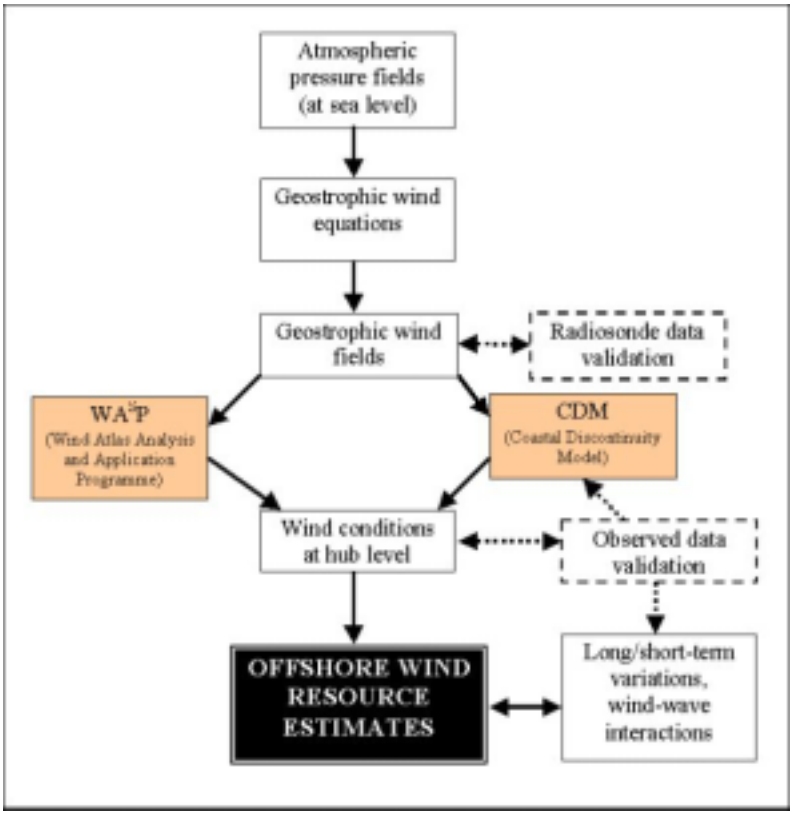

Figure 1. A schematic of the POWER methodology [Source: Watson *et al*, 1999].

* Further information about the POWER project can be found at the web site:
http://www.eru.rl.ac.uk/power_project/power_project.htm

The main advantage of the POWER methodology is the use of MSLP data. This can be considered roughly homogeneous over time and space due to the uniformity of methods used to measure pressure (Palutikof *et al*, 1997). It allows both short and long-term wind speed variability to be examined and therefore predicted. A disadvantage is that the grid squares used for the pressure datasets have a low resolution (2.5^o to 10^o). However, the MSLP gradient can be reliably interpolated to a 0.5^o grid square (Watson *et al*, 1999).

1.4 LONG-TERM VARIABILITY IN WIND SPEEDS

The long-term variability of wind speeds has been investigated above mainland locations and interdecadal change has been found to be significant to wind energy economics. For example, Palutikof *et al* (1987) examined wind speed records at Southport from 1898-1954. The annual mean varied between 5.2 ms^{-1} (1899 and 1945) and 7.3 ms^{-1} (1923), representing a possible 50% change in power output as the power generated is proportional to the cube of the wind speed (BWEA, 2000). They conclude that long-term variability in the wind field exists on a scale significant to the wind energy industry.

MSLP datasets are now available that provide a comprehensive spatial and temporal distribution (Ward & Hoskins, 1995). By adopting the geostrophic wind method, historical data can be analysed retrospectively data back to the late 19^{th} century. This provides a considerable opportunity to examine long-term variation in wind fields, reflecting either natural climate variability or climate change. Recognition of the potential change in a wind resource over a 20-25 year period (the average lifespan of a wind turbine (BWEA, 2000)) will aid the determination of the most economically viable offshore wind farm locations.

The geostrophic wind method has also been used to examine long-term variability in onshore wind speeds (Palutikof *et al*, 1992), revealing possible implications for wind energy resources. For example, the mean wind speed at High Bradfield ranged from 6.9 ms^{-1} (1930-50) to 7.3 ms^{-1} (1880-1900).

The European Wave and Storms in the North Atlantic (WASA) project has detected a change in ocean wind fields, concluding that the storm and wave climate of the North Sea and North East Atlantic has shown significant interdecadal variability (Carretero *et al*, 1998). Investigation of the offshore trend throughout the last century has not yet been undertaken.

1.5 THE NORTH ATLANTIC OSCILLATION

The NAO is a key mode of climate variability in the northern hemisphere (Stephenson *et al*, 2000). It exhibits interannual and interdecadal variability that mainly affects temperature, precipitation and wind fields over North America, Europe and North Africa (Mehta *et al*, 1999). The NAO index can be defined as the pressure difference between the normalised SLP at a station in Gibraltar and the normalised SLP at a station in South-west Iceland (Jones *et al*, 1997).

The strongest variability is in winter so the most useful NOA index has been derived from December to March (Osborn *et al*, 1999). High NAO winters, common from the 1980s to 1990s, are associated with strong surface westerlies blowing from the North Atlantic across Europe. This leads to warmer than usual winter temperature over much of Europe. Hurrell (1995) states that low NAO winters (such as those experienced from the 1940s to 1970s) can result in westerlies up to 8 ms^{-1} weaker than the opposite mode. Whilst interannual variability is strong there is also persistence in the NAO that leads to anomalously high or low modes on a decadal scale.

The NAO is poorly understood, with various mechanisms being suggested for its variability. Unlike the El Niño Southern Oscillation (ENSO) phenomenon the NAO has no clear periodicity and may be forced by oceanic or atmospheric processes (Uppenbrink, 1999). Rodwell *et al* (1999) believe that the sea surface temperature is driving the atmospheric changes through evaporation, precipitation and atmospheric heating. Osborn *et al* (1999) used Hadley Centre HadCM2 climate model results to predict future NAO behaviour. They conclude that the early 21st century is likely to exhibit a weakening in the winter pressure gradient between Iceland and Gibraltar, leading to weaker westerlies and resulting lower temperatures (such regional cooling may be offset by anthropogenic climate change). The NAO dataset from 1821 is available from the University of East Anglia (UEA) Climatic Research Unit (CRU, 2000) web site as plotted in figure 2.

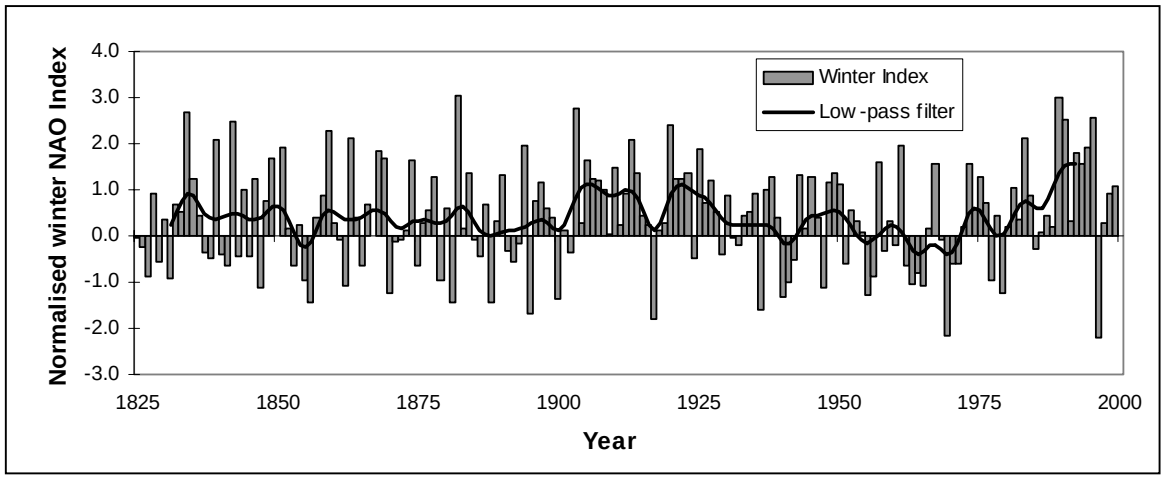

Figure 2. The winter NAO index (Dec-March) from 1821-1999 [Data source: CRU, 2000].

1.6 SUMMARY

This review of the field has demonstrated that an investigation into the long-term variability of offshore wind speeds is required. The geostrophic transformation provides an appropriate tool for converting MSLP data into mean wind speeds. The transformed data can then be statistically analysed for interdecadal variability in offshore wind speeds. Associations between wind speeds and the NAO may reveal trends in the offshore wind resource that are linked with a major climatological mode over European oceans.

1.7 HYPOTHESIS, AIMS AND OBJECTIVES

This study will investigate the hypothesis:

> **The interdecadal variability in offshore wind speeds significantly affects power generation from offshore wind turbines.**

The central aim of this study is to examine the long-term variability in offshore wind speeds.

Six key objectives are identified in order to achieve this aim are to:

- Calculate sea surface wind speeds for European waters using the historical UK Meteorological Office (UKMO) MSLP dataset.
- Verify the homogeneity and accuracy of the UKMO pressure data and the derived winds by comparison of surface winds with US National Centers for Environmental Prediction / National Center for Atmospheric Research (NCEP/NCAR) wind speeds.
- Compare the calculated surface winds with reliable offshore wind measurements.
- Statistically analyse the newly calculated and NCEP/NCAR wind speeds to examine how sea surface winds vary on an interannual to interdecadal scale.
- Interpret the data and perform further statistical analysis to examine possible links with the NAO.
- Relate any findings to the viability of wind energy production at offshore locations.

2. METHODS AND DATA

This section defines the methodology used to calculate wind speeds over European waters at wind turbine hub heights. The choice of datasets is justified and modifications to the original method are discussed. Statistical techniques used to describe and analyse the data are explained.

2.1 METHODS TO CALCULATE WIND SPEEDS

2.1.1 GEOSTROPHIC WIND SPEEDS

Observations of the 'free atmosphere' (above the *friction layer*, normally 500-1000 metres above ground) have shown that the wind blows at right angles to the pressure gradient. In the Northern Hemisphere high pressure lies to the right of this free atmosphere wind, known theoretically as the geostrophic wind (Barry & Chorley, 1998). The MSLP data will be converted to the geostrophic wind using the equations:

$$V_g = -\frac{1}{f\rho} \cdot \frac{\delta p}{\delta n} \qquad \text{(Eq. 2.1)} \qquad \text{(Stull, 1988)}$$

Where $\mathbf{V_g}$ is the geostrophic wind, $\boldsymbol{\rho}$ is the density of the air (1.225 kg m^{-3} at 15°c and standard surface pressure (Seinfeld & Pandis, 1998)), $\boldsymbol{f}$ is the coriolis parameter, and $\boldsymbol{\delta p/\delta n}$ is the change in pressure in the horizontal plane. The distance $\boldsymbol{\delta n}$ between two lines of longitude will change with latitude. This is calculated from the radius of the Earth (6.37 x 10^6 m (Serway, 1996)) and $\boldsymbol{\theta}$, the angle of latitude.

The coriolis parameter is defined as:

$$f = 2.\omega.\sin\theta \qquad \text{(Eq. 2.2)} \qquad \text{(Barry \& Chorley, 1998)}$$

Where $\boldsymbol{\omega}$ is the angular rotation of the Earth (7.27 x 10^{-5} radians s^{-1}).

2.1.2 PRESSURE GRADIENTS

Palutikof and Holt (2000) use a 2° spacing in the north-south direction and a 4° spacing in the east-west direction to calculate pressure gradients on the grounds that the geostrophic wind reflects relatively large-scale processes. The longitudinal grid spacing is twice that of the latitudinal spacing to balance the decrease in the east-west distance whilst moving poleward from the equator. This method is adopted here to calculate the 'u' and 'v' components of the geostrophic wind. These are calculated and then converted to surface wind speeds and then combined to a scalar quantity (the overall wind speed).

NCEP/NCAR daily MSLP data from recent years has been used by Palutikof and Holt (2000) to calculate geostrophic wind speeds for 1/1/90 and 26/1/90. The same daily geostrophic wind speeds were calculated from the NCEP/NCAR data using the method described in equation (2.1). Geostrophic wind speeds produced here were almost identical to those of Palutikof and Holt. The slight differences are due to interpolation methods.

2.1.3 SURFACE WIND SPEEDS

The relationship between the geostrophic wind and the surface wind is complex, involving effects from surface roughness and atmospheric stability. An approximate description is that the wind turns to the left (in the Northern Hemisphere) and slows by approximately one-third as it approaches the ocean surface (Barry & Chorley, 1998).

The friction velocity has been shown to be related to $\mathbf{u_z}$, the wind at height **z** above the surface, and the surface roughness, $\boldsymbol{z_0}$ (taken as 0.0002 for open ocean (Stull, 1988)), by the relationship:

$$u_z = \frac{u_*}{\kappa}.\ln\left(\frac{z}{z_0}\right) \qquad \text{(Eq. 2.3)} \qquad \text{(Troen \& Petersen, 1989)}$$

Equation (2.3) describes the logarithmic wind speed profile that has been shown to quite accurately simulate the change in wind speed with height. This is used to convert wind speeds to various hub heights in this study.

The relationship between the friction velocity (u_*) and the geostrophic wind speed is described by the geostrophic drag law:

$$V_g = \frac{u_*}{\kappa}\sqrt{\left[\ln\left(\frac{u_*}{fz_0}\right) - A\right]^2 + B^2} \qquad \text{(Eq. 2.4)} \qquad \text{(Troen \& Petersen, 1989)}$$

Where κ is the is the von Kármán constant (taken as 0.40), and $\boldsymbol{A}$ and $\boldsymbol{B}$ are constants with values of 1.8 and 4.5 respectively (Troen & Petersen, 1989).

Equation (2.4) was investigated using a range of initial values for the friction velocity and calculating the geostrophic wind speed. Latitude was kept constant at 50° N so the coriolis parameter remained constant. The correlation between the geostrophic wind speed and the friction velocity was found to be almost linear at constant latitude and surface roughness. However, the correlation coefficient (R^2) is less than 1, revealing that there is not an exact linear relationship. Other curve

types were fitted to the data and these are compared in table 1. A power relationship obtained the highest R^2 value and was chosen for this work.

Table 1. A comparison of curves to describe the relationship between friction velocity and geostrophic wind speed.

Type of curve	Equation	Correlation (R^2)
Linear	$u_* = 0.02296Vg + 0.04313$	0.99966
Polynomial	$u_* = -0.00002Vg^2 + 0.02450Vg + 0.01828$	0.99997
Power	$u_* = 0.03028\ Vg^{0.94131}$	**0.99999 [Best fit]**

Further investigation found that the fit of the curve could be improved by varying the power curve slightly as the geostrophic wind increases. Ideally a set of curves should be used for each latitude. However, adapting the relationship for bands of 5° latitude was found to produce errors of less than 1%. For example the equation derived at 32.5° N is used from 30° to 35° N. Eight bands are used in total. The above procedure is employed to minimise the error from the equation (2.4) but due to other assumptions the surface winds are unlikely to be within 1% of actual observed wind speeds.

2.1.4 WIND TURBINE HUB HEIGHTS

In order to apply wind speeds to energy potential they must be calculated at the hub height of wind turbines. These vary depending on design and power output but are likely to increase as the technology progresses (Border Wind, 1998). The British Wind Energy Association (BWEA, 2000) give the current range of offshore turbine heights as 25-80 metres, the upper limit of 80 m is used in this study.

2.1.5 WIND DIRECTION

The analysis of wind direction is beyond the scope of this work. The identification of suitable areas for siting wind turbines would be followed by in-situ measurements of the prevailing wind direction to maximise the positioning relative to the wind.

2.1.6 ASSUMPTIONS AND SIMPLIFICATIONS OF THE MODEL

The model described above has been chosen because of limitations on the availability of data. However, for use on the open ocean it is believed that the method will obtain suitably accurate results (Troen & Petersen, 1989). The main assumptions involve sea surface roughness length and stability whilst coastal effects are not considered.

The assumption that the sea surface roughness can be taken as constant is a simplification because there is interaction between wind and waves (Lange & Højstrup, 1999). High wind speeds will

increase the wave height and in turn the surface roughness, which will slow the surface winds. Charnock's formula relates surface roughness to the friction velocity:

$$z_0 = a\frac{u_*^2}{g} \qquad \text{(Eq. 2.5)} \qquad \text{(Troen \& Petersen, 1989)}$$

Where a = 0.114 and g = acceleration due to gravity (9.8 ms^{-2}).

Equation (2.5) can be used once the friction velocity has been calculated and the new value of the surface roughness can be fed back into equation (2.4). Iteration of equations (2.3), (2.4) and (2.5) would lead to improved values for z_0 and u_* (Barthelmie, 1991). This relationship has not been incorporated into this work for two reasons. Firstly, the European Wind Atlas (Troen & Petersen, 1989) states that the constant surface roughness method obtains very similar results to the iterative method with regards to the moderate and high wind speeds of interest to offshore wind energy. Secondly, the computational time might hinder other more important parts of the analysis.

Stability cannot be calculated due to the lack of temperature profile data so neutral stability is assumed throughout. Coastal effects such as fetch will be ignored by focusing on only the open ocean.

The model was tested initially by calculations using a spreadsheet but the final programme was written in Fortran 77. MSLP data is read from a file in 4 year periods (due to limited disk space) and daily wind speeds are outputted. The programme is listed in Appendix 2.

2.2 CHOICE OF DATASETS

2.2.1 UKMO DAILY MEAN SEA LEVEL PRESSURE (MSLP)

The creation of a suitable long-term wind speed dataset requires pressure data for more than a century. The UKMO MSLP dataset is a climatic data series widely used in research (Jones, 1987). The daily data has a spatial coverage of 15° N to the North Pole at a 10° longitude by 5° latitude grid resolution dating from November 1880 to May 1995. Many sources were used to create the dataset and this has led to problems with homogeneity (see Palutikof *et al*, 1992). These are considered further on page ****. The dataset is incomplete over the spatial domain of this study (15° W – 30° E; 30° N – 70° N) for parts of the time series and particularly above 61° N. Only full years are considered here so the temporal range is shortened to 1881-1995. Wind speeds calculated from the UKMO MSLP data are known from hereon as the *derived* wind speeds.

2.2.2 NCEP/NCAR MONTHLY MEAN 10 m WIND SPEEDS

In 1991, NCEP and NCAR began a Reanalysis Project using state-of-the-art analysis/forecast systems and a wide range of data inputs to produce a global dataset of atmospheric variables (Kalnay *et al*, 1996). The model simulates 1 month (run-time) per day (real-time) and has now been used to create data from 1948-2000. The aim of the project is to allow research into climatic changes on a relatively long-term scale. Principal data sources are listed in table 2.

Table 2. NCEP/NCAR Reanalysis data sources [Source: Kalnay *et al*, 1996].

Dataset	**Description / comments**
Global rawinsonde data	Upper air observations
Comprehensive Ocean-Atmosphere Dataset (see Woodruff *et al,* 1998) surface marine data	From buoys, ships, observation stations etc.
Aircraft data	Aeroplanes and constant pressure balloons
Surface land synoptic data	-
Satellite sounder data	From the late 1960s and early 1970s
Satellite cloud drift data	From 1978-91

NCEP/NCAR MSLP data was initially considered appropriate for calculating wind speeds using the same method applied to the UKMO MSLP record. However, the reliable NCEP/NCAR MSLP dataset is significantly shorter than their wind speed dataset due to a problem with the encoding of MSLP data from 1948-67 (CDC, 2000). For this reason the pressure data quality is questionable up to 1967. European observations were worst affected by the problem (CDC, 2000). Therefore the monthly wind speeds produced by the NCEP/NCAR Reanalysis Project are considered the most appropriate secondary dataset.

A comparison of the derived monthly surface wind speeds and those calculated by NCEP/NCAR are used to examine homogeneity and the general trend in the long-term data.

2.2.3 DATA ACQUISITION

Daily MSLPs from the UKMO dataset were obtained from the CRU for the domain of 20° W - 40°E and 25° N - 75° N. The extended grid is required for accurate interpolation to the boundaries. NCEP/NCAR monthly 10 m wind speeds were obtained from the Climate Diagnostics Center* web site and the spatial domain extracted. The NAO winter index was downloaded from the CRU web site (CRU, 2000).

***** NCEP/NCAR Reanalysis data was provided by the NOAA-CIRES Climate Diagnostics Center, Boulder, Colorado, USA, from their Web site at http://www.cdc.noaa.gov/. The monthly mean surface wind speed dataset can be found obtained by file transfer protocol at: ftp://ftp.cdc.noaa.gov/Datasets/ncep.reanalysis.derived/surface/wspd.mon.mean.nc

2.3 DATA TRANSFORMATION

2.3.1 INTERPOLATION OF THE DAILY PRESSURE GRID

The Grid Analysis and Display System* (GrADS) was used to interpolate the datasets from a coarse to a fine grid. The package provides 4 possible interpolation functions, the most complex of which is the 4-point bessel method. This considered the most appropriate method for this work because higher-order terms in the polynomial interpolation function are capable of producing a close match to the original data in regions of rapid change (Fiorino, 1995). This method should be capable of modelling pressure gradients such as those around low pressure centres.

Similar manipulation of pressure data has been performed by Palutikof and Holt (2000) using two other methods, bicubic and bicubic spline interpolation, discussed in detail by Press *et al* (1997). Geostrophic wind speeds over Western Europe obtained here using bessel interpolation were compared to those obtained by the alternative methods and the results were found to be very similar, confirming the suitability of the choice of method. The interpolations are discussed below for each dataset.

2.3.2 NCEP/NCAR WIND SPEEDS

The NCEP/NCAR monthly mean wind speeds are calculated by combining the 6-hourly 'u' and 'v' wind vectors to a scalar quantity. The scalar wind is then averaged to produce a monthly mean at each grid point (Hooper, 2000).

The NCEP/NCAR grid resolution is 2.5º x 2.5º. The chosen fine resolution for this work is 0.5º x 0.5º, equivalent to a 35.7 km (east-west) x 55.6 km (north-south) box at 50º N. Figure 3 shows the original and post-interpolation (0.5º x 0.5º) wind speed contour plots for January 1948 wind speeds. The pattern is similar but the interpolated grid produces a smoother, more realistic set of contours than the original plot. The monthly wind speeds are already averaged so large gradients over short distances do not exist, as a result errors due to interpolation are likely to be minimal. There is good agreement between the plots, indicating that the bessel function is not distorting the dataset or introducing significant errors.

* The Grid Analysis and Display System* (GrADS) is an interactive manipulation and display package for spatially distributed data. It is freely available via the Internet at http://dao.gsfc.nasa.gov/software/grads/win32/latest/ and is currently used worldwide for the analysis and display of earth science data.

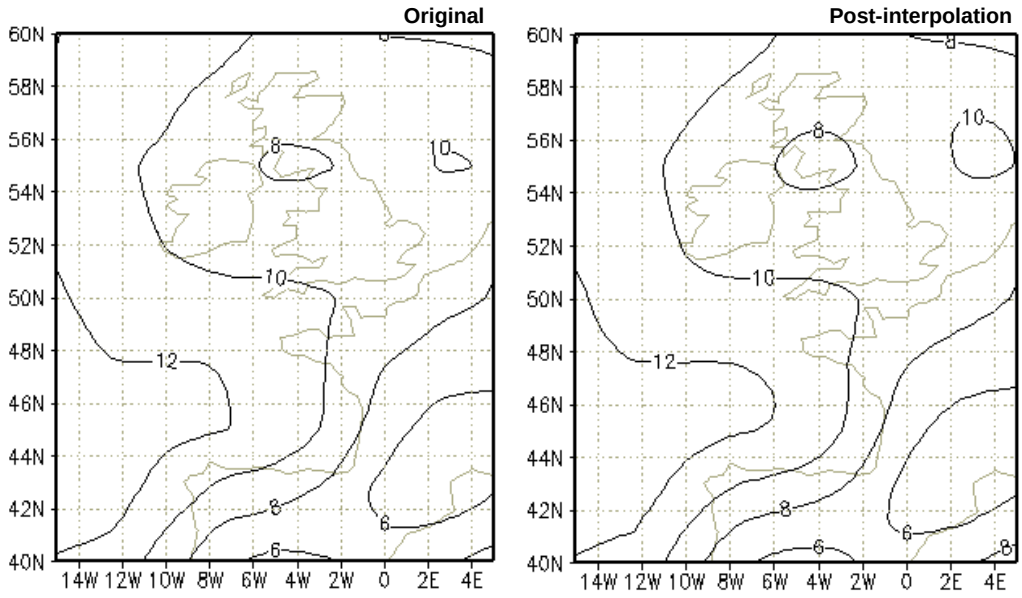

Figure 3. Original and post-interpolated NCEP/NCAR monthly wind speeds for January 1948 over the UK.

2.3.3 UKMO MSLP

The daily MSLP data was interpolated before wind speed calculations or averaging were performed. The MSLP is a synoptic scale atmospheric variable whereas wind speed is a derivative of the pressure. Therefore the MSLP data can be interpolated more meaningfully because it exhibits both larger spatial and longer temporal characteristics that will not be significantly altered by interpolating to a finer grid. Watson *et al* (1999) propose that the shortest time step available (daily) should be used to ensure that the effect of short-term variability is not smoothed in the wind calculations.

The interpolation of the monthly NCEP/NCAR wind speeds was calculated from a higher resolution grid than the UKMO data, reducing the likelihood that interpolation will lead to significant errors.

2.3.4 MODIFYING THE INTERPOLATION METHOD

Initial interpolations of the UKMO data led to anomalously high wind speed peaks that were spatially correlated with the original 10º x 5º grid points. Investigation of the cause found that the transition from the coarse to the fine grid was creating discontinuities in the MSLP data due to the bessel function. A two-step interpolation to a 2.5° x 2.5° and then 0.5° x 0.5° grid removed the anomalies. Both interpolations maintained the integrity of the previous grid whilst smoothing the curves between points.

2.3.5 CHECKING THE INTERPOLATED MSLPs

The interpolated MSLP grids for 6 randomly chosen days were compared with Royal Meteorological Society UK Weather Log SLP. The comparison showed good agreement, confirming that the interpolated MSLPs used in this work were representative of the synoptic pressure conditions.

2.4 STATISTICAL METHODS

2.4.1 LINEAR REGRESSION AND COMPARISON OF MEANS

Linear regression analysis is applied to the derived, NCEP/NCAR and NAO datasets. Bivariate correlations are examined and coefficients of determination (R^2) are obtained using the SPSS 9.0.0 for Windows statistical package. R^2 values provide a measure of the linear relationship between two variables, where a value of zero shows no correlation and one gives represents perfect correlation (Haber & Runyon, 1973). The difference in the means between two datasets was tested for statistical significance using a comparison of means test.

2.4.2 LOW-PASS FILTERING

To observe the long-term trend in a time series by suppressing short-term variability a low-pass filter can be applied (Kotz & Johnson, 1985). All low-pass filters used in this work have a period of 15 years with weightings calculated from a Normal distribution.

3. RESULTS

Derived wind speeds are compared to observations and NCEP/NCAR Reanalysis data. The datasets are found to broadly agree and the highest correlation is in the north-west over open ocean. Correlations with the North Atlantic Oscillation are greatest over the same region. The NCEP/NCAR data is used to correct an anomaly in the derived wind speeds.

3.1 ADJUSTMENT OF THE START YEAR TO 1883

The analysis highlighted two anomalous periods in the UKMO MSLP dataset that are detailed in Appendix 3 (page **). The first anomaly raises doubts over the accuracy of the 1882 data so the results will only present wind speeds from 1883-1995.

3.2 COMPARISONS OF THE MODEL OUTPUT WITH WIND SPEEDS MEASUREMENTS

An initial test of the method was undertaken by comparing modelled wind speeds with observational data in the literature. Barthelmie (1991) lists long-term mean values at a 20 m height at three offshore locations. These are Bell Rock (2.24° W, 56.26° N), West Sole (1.15° E, 53.82° N) and Data Buoy 1 (8.97° W, 48.72° N). Table 3 compares results obtained here with measured wind speeds and those obtained from alternative models.

Table 3. Observed and modelled mean wind speeds at 20 m height (ms^{-1}).

Location	Data Period	Averaging time	Observations	Børresen (1987)	Barthelmie* (1991)	Derived in this study	% error**
Bell Rock	1971-80	Annual	7.5	8.9	7.6	8.1	8.0
		Winter	8.7	10.9	8.9	10.1	16.1
		Spring	6.8	8.5	7.4	7.4	8.8
		Summer	5.8	6.7	6.3	5.7	-1.7
		Autumn	8.4	9.8	8.5	9.0	7.1
West Sole	1983-85	Annual	8.4	8.6	8.1	7.9	-6.0
		Winter	10.9	10.5	9.0	10.3	-5.5
		Spring	7.6	8.5	7.6	6.8	-10.5
		Summer	6.0	6.7	6.5	6.1	1.7
		Autumn	9.8	9.3	8.5	8.5	-7.1
Data Buoy 1	1978-82	Annual	9.2	9.1	9.2	7.6	-17.4
		Winter	10.1	10.9	10.8	9.1	-9.9
		Spring	9.6	8.8	8.8	7.8	-18.8
		Summer	7.9	7.0	7.5	6.1	-9.8
		Autumn	9.3	9.0	9.3	7.6	-18.3

* The best results were obtained from Barthelmie's improvement to Moore's 900 mb model.
** The percentage error is calculated as the difference in between the derived and observed wind speed divided by the observed wind speed multiplied by 100.

It is clear that the model does not exactly replicate measured values. The annual percentage error varied between 6% lower than the observed mean wind speed (West Sole) and 17% lower than observed (Data Buoy 1). However, the seasonal averages of Barthelmie's (1991) model also differ from observations by up to 1.9 ms^{-1} (17% below the observed mean winter wind speed at West Sole). The results would not be expected to match exactly since the grid resolution is limited to 0.5°.

3.3 COMPARING DERIVED AND NCEP/NCAR WIND SPEEDS

3.3.1 GENERAL TRENDS

Monthly mean 10 m wind speeds were calculated from 1948-95 for comparison with the NCEP/NCAR data. In any month, the wind was left undefined if more than 11 days of data were missing. The datasets are summarised in figures 4 to 6, showing the 1948-95 long-term mean, monthly and annual standard deviations for the derived and NCEP/NCAR wind speeds.

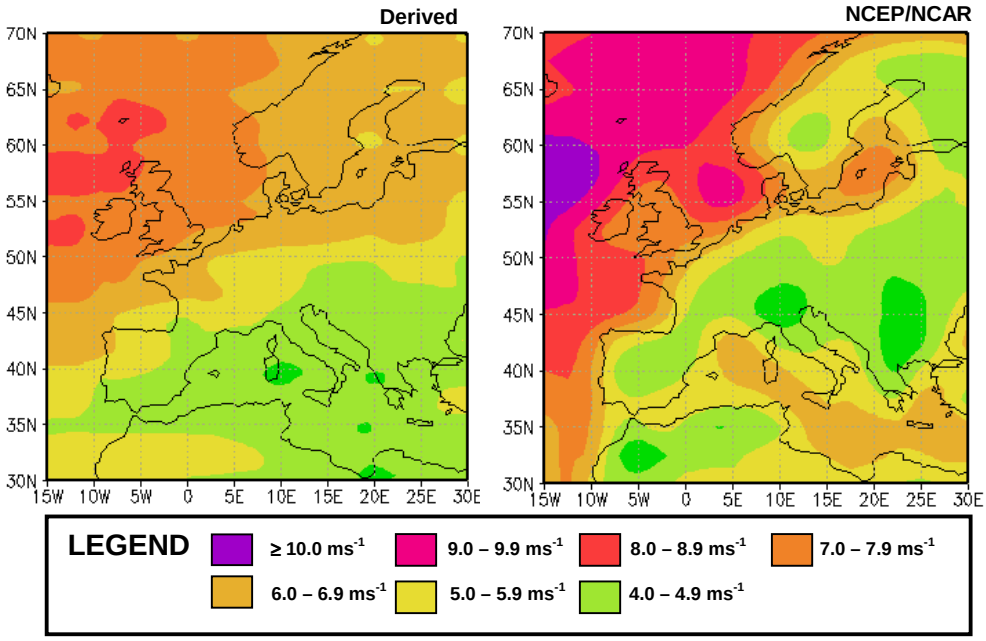

Figure 4. Annual long-term means for derived and NCEP/NCAR datasets from 1948-95.

It is clear that the patterns are different over the landmass for each dataset, the NCEP/NCAR data shows pronounced wind speed gradients over the coastal regions. This is not significant to this study because only wind speeds above European waters are of interest.

The spatial trends of the long-term means are similar with strong winds over the Atlantic and lighter winds over the landmass and Mediterranean. The NCEP/NCAR wind speeds are faster over most of the Atlantic region and both datasets show a maximum to the west of Scotland. The logarithmic wind profile can be used to adjust the 10 m winds to other hub heights.

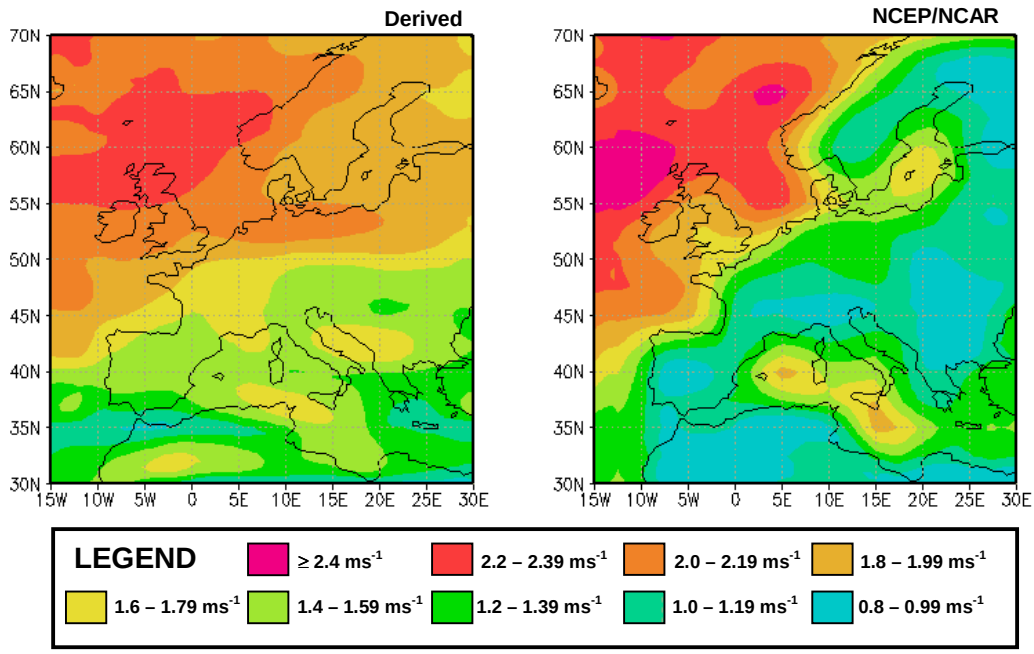

Figure 5. Monthly standard deviations for derived and NCEP/NCAR datasets showing the seasonal and interannual variability from 1948-95.

The spatial patterns of the monthly standard deviations (figure 5) reflect the long-term mean patterns with the highest variability to the north-west of the British Isles (>2.4 ms^{-1}). The NCEP/NCAR plot shows a greater range of monthly variability than the derived data including steeper gradients where the ocean meets land. This pattern shows the lowest standard deviations (0.8 - 0.99 ms^{-1}) mirroring the lowest means over the landmass.

The lowest variability in the derived annual standard deviations is over both land and sea (0.8 - 0.99 ms^{-1}), located along the 35°N band. These are areas of relatively low wind speed where the moderate climate reduces the seasonal variability.

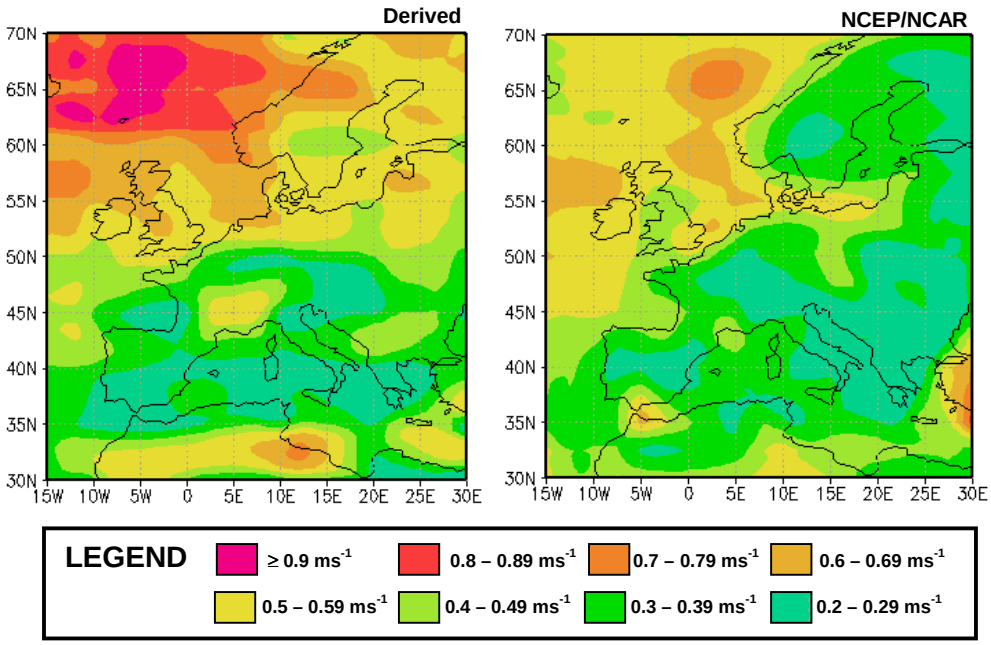

Figure 6. Annual standard deviations for derived and NCEP/NCAR datasets showing the interannual variability.

The annual standard deviations (figure 6) show greater variability in the NCEP/NCAR data with a range of 0.2 ms^{-1} (Mediterranean) to over 0.9 ms^{-1} (east of Iceland). The pattern is lower to the south-east with significant local increases over the Gibraltar Strait and the Eastern Mediterranean. The lower maxima in figure 6 compared to figure 5 reflect the removal of the seasonal cycle which generally shows higher wind speeds in winter, increasing the variability by a factor of 3 in some locations.

The high variability over Northern Africa in both derived standard deviations is not discussed here as winds over land are not accurately modelled.

3.3.2 COMPARISON OF MEANS AND CORRELATIONS

Data was extracted for 16 randomly chosen grid points (see figure 7) in order to examine the correlation between the monthly mean derived and NCEP/NCAR wind speeds. The whole spatial grid was not examined because it consists of 7371 points at each monthly time step.

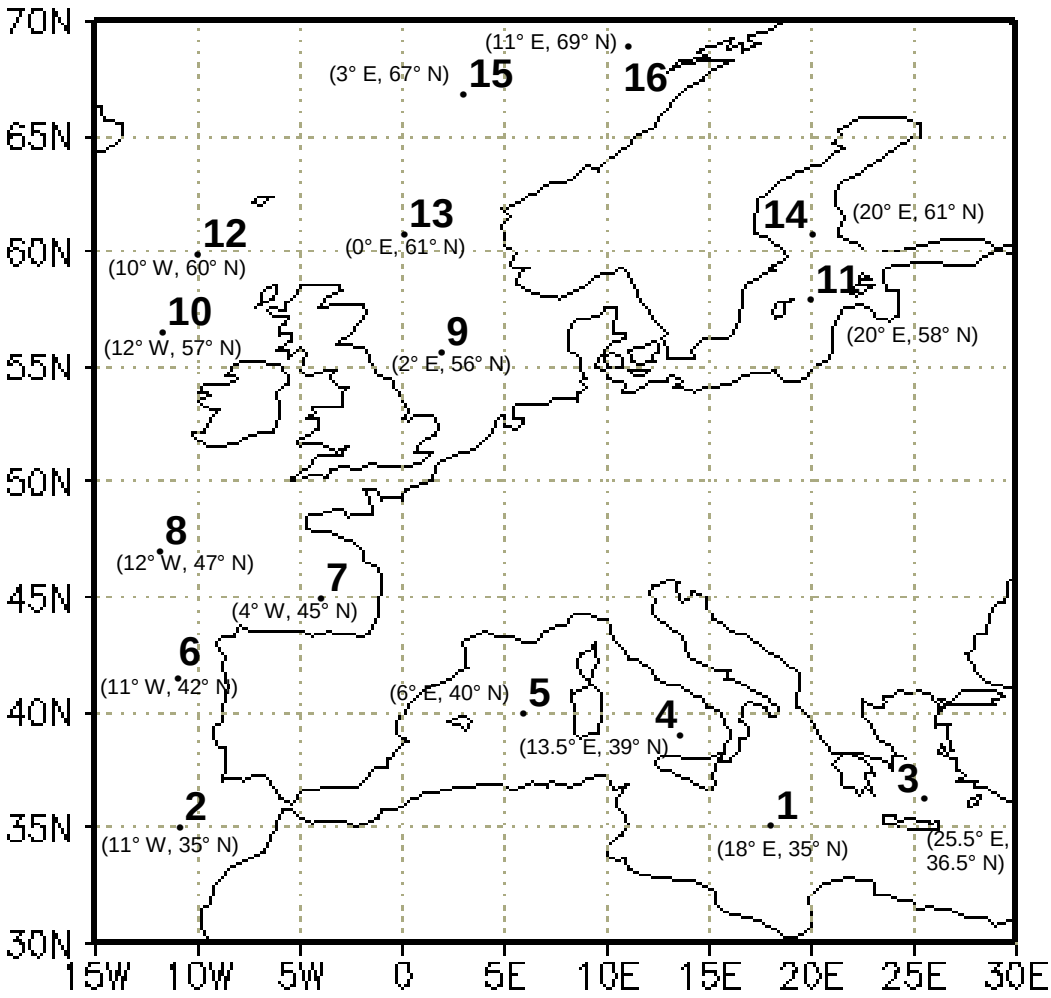

Figure 7. The locations of grid points 1-16

A comparison of means test was performed at each grid point. The summary statistics for each dataset and difference in means are presented in table 4. The NCEP/NCAR winds were consistently higher by an average of 1.8 ms^{-1}.

Table 4. Summary statistics and difference in means for the derived and NCEP/NCAR monthly mean 10 m wind speeds at grid points 1-16.

1948-95: DERIVED WIND SPEEDS																	
	1	**2**	**3**	**4**	**5**	**6**	**7**	**8**	**9**	**10**	**11**	**12**	**13**	**14**	**15**	**16**	**MEAN**
AVERAGE	4.0	4.8	4.9	4.1	4.1	6.5	5.6	7.5	7.2	8.6	6.5	7.8	7.5	6.0	7.5	6.6	6.2
MAX	9.0	8.1	8.2	8.3	8.6	13.1	10.8	14.6	14.7	15.4	11.9	14.4	15.0	10.8	13.2	12.8	-
MIN	2.0	2.7	2.5	1.6	1.7	3.0	2.8	3.7	3.4	3.6	2.7	3.0	3.0	2.4	3.7	3.2	-
RANGE	7.0	5.3	5.7	6.7	6.8	10.0	8.0	11.0	11.3	11.7	9.1	11.4	12.0	8.4	9.5	9.6	9.0
S.D.*	1.3	0.9	1.0	1.3	1.4	1.6	1.5	1.9	1.9	2.1	1.7	2.0	2.0	1.7	2.0	1.7	1.6
1948-95: NCEP/NCAR WIND SPEEDS																	
	1	**2**	**3**	**4**	**5**	**6**	**7**	**8**	**9**	**10**	**11**	**12**	**13**	**14**	**15**	**16**	**MEAN**
AVERAGE	6.5	7.2	6.5	5.8	6.4	7.9	7.2	9.0	9.2	10.6	7.8	10.0	9.2	6.6	9.4	8.3	8.0
MAX	12.2	11.1	9.7	10.8	12.1	12.8	12.3	16.6	16.8	18.9	13.2	17.0	16.5	10.9	15.5	14.9	-
MIN	3.4	4.7	3.3	2.9	3.3	4.3	4.2	5.1	4.9	5.6	4.3	5.5	4.0	3.4	4.8	4.6	-
RANGE	8.9	6.4	6.3	7.9	8.7	8.5	8.1	11.5	11.9	13.3	8.9	11.5	12.5	7.4	10.7	10.3	9.6
S.D.	1.5	1.1	1.1	1.4	1.6	1.4	1.6	2.0	2.1	2.4	1.6	2.3	2.1	1.3	2.1	1.8	1.7
DIFFERENCE IN MEANS (1948-95)**																	
	1	**2**	**3**	**4**	**5**	**6**	**7**	**8**	**9**	**10**	**11**	**12**	**13**	**14**	**15**	**16**	**MEAN**
NCEP/NCAR *minus* Derived	2.5	2.4	1.7	1.7	2.2	1.3	1.7	1.6	2.0	2.0	1.3	2.2	1.7	0.6	1.9	1.8	1.8

* S.D. – standard deviation *(n-1)*.
** All significant at the 95% confidence level.

3.3.3 INTERANNUAL VARIABILITY

Interannual variability was examined using grouped monthly data. The average coefficients of determination (R^2) for each month across all grid points is shown in figure 8.

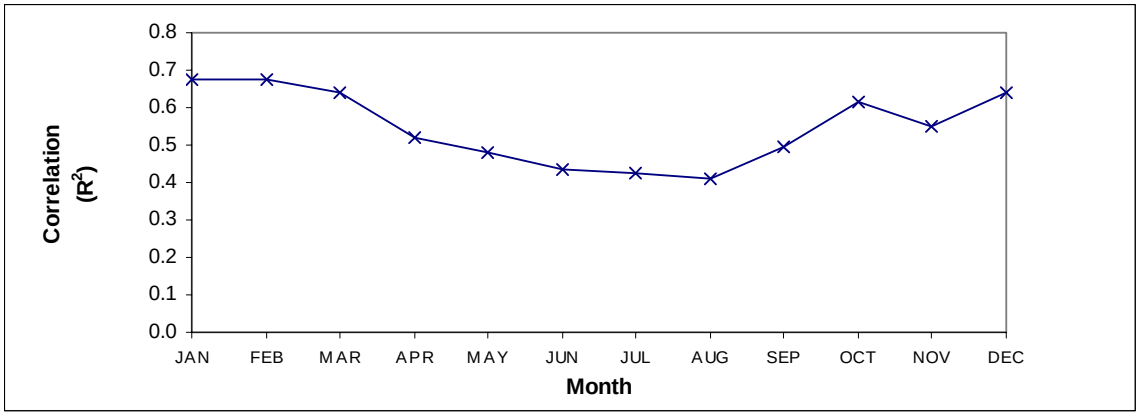

Figure 8. Mean monthly R^2 values correlating NCEP and derived data averaged across 16 grid points from 1948-95.

January and December showed the strongest correlations between the two datasets with mean R^2 values of 0.68 and 0.64 respectively. The highest individual correlation was found at grid point 7 for February (0.84) and the lowest was at grid point 3 for June (0.09). Wind speeds generally peak in winter, suggesting that there is less correlation when mean wind speeds are lower. The seasonal cycle varies considerably across the spatial domain, this is discussed in Appendix 4 (page ***).

The correlation between the monthly mean datasets was also investigated without grouping the months. This method includes the correlation of the seasonal cycle and therefore resulted in higher R^2 values ranging from 0.51 at grid point 3 to 0.88 at grid point 9 with a mean of 0.78. A 5° x 5° resolution grid of monthly mean data was extracted to examine the spatial pattern of correlation between the datasets (see figure 9).

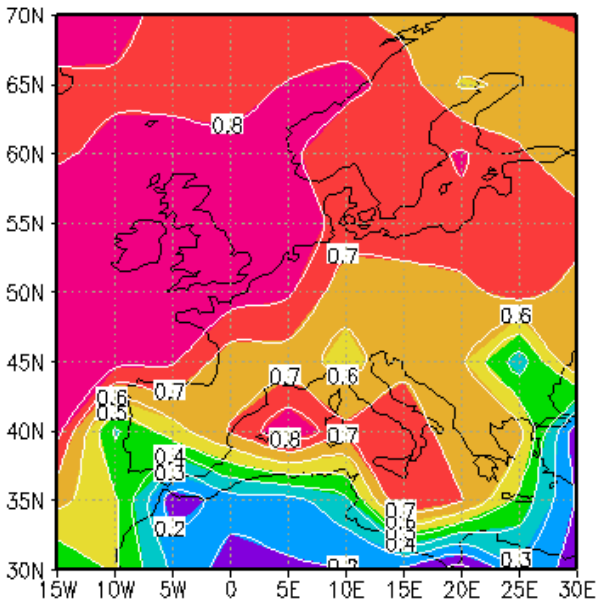

Figure 9. A contour plot of the correlation between the monthly mean derived and NCEP/NCAR wind speeds.

The correlation is highest over the open ocean (>0.7) and parts of the Mediterranean. There is less agreement towards the south-east sector where the correlation is reduced significantly (<0.2). However, most of the Mediterranean has an R^2 value of over 0.5.

3.4 CORRELATIONS BETWEEN WIND SPEEDS AND THE NAO

Linear correlation was examined between the winter NAO index and both wind speed datasets using winter means (December-March) for each year from 1948-95. The highest correlations were found in the North Atlantic and the North Sea. Figure 10 shows how the derived data correlates slightly higher than the NCEP/NCAR data with the NAO. Comparisons using a low-pass filter produced lower correlation coefficients.

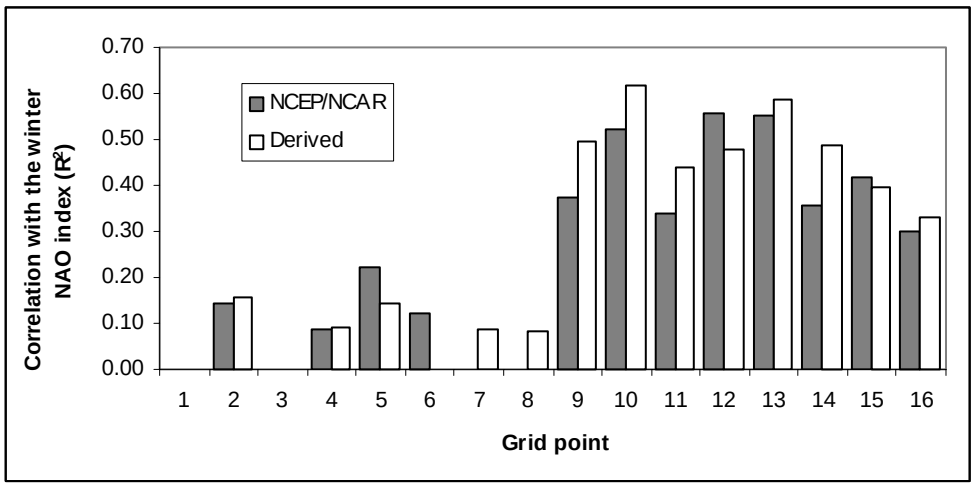

Figure 10. A bar chart showing R^2 values for the correlation of derived and NCEP/NCAR datasets with the NAO index. The bars are omitted where the correlation was not significant at the 95% confidence level.

A visual examination of the NAO and wind speed plots suggested that the correlation has improved in recent years. A 21-year running correlation was therefore performed and the period from 1883-1995 was used for the derived data. Grid points 15 and 16 were not tested because of missing data over much of the time series. Of the other 14 grid points, 6 showed no discernible trend whilst grid points 9-14 all exhibited a positive trend from the mid-1960s to the mid-1980s (as recent as the 21-year correlation could measure). Figure 11 illustrates this for both datasets at grid point 9.

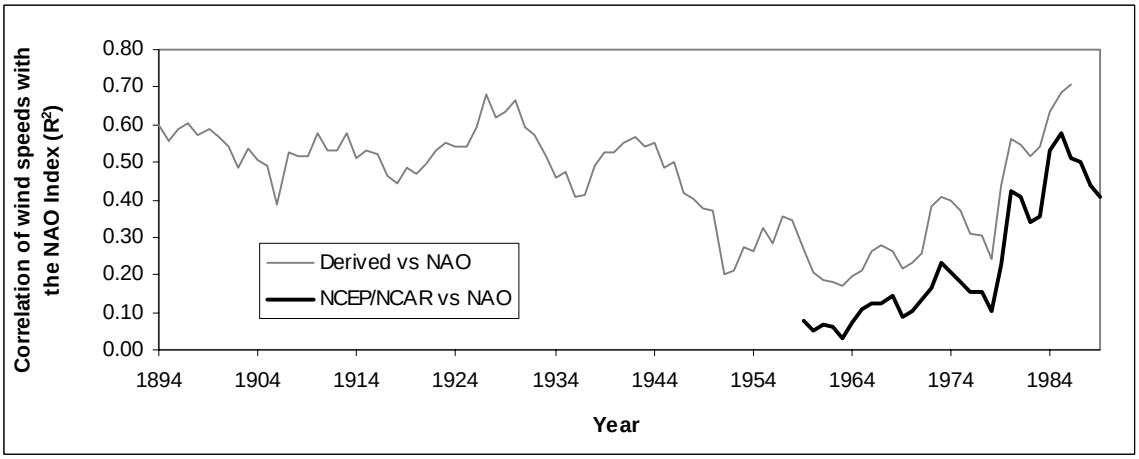

Figure 11. A 21-year running correlation between the NAO index and mean winter 10 m wind speeds at grid point 9.

3.5 TIME SERIES ANALYSIS

Annual means were calculated from the monthly mean 10 m wind speeds for both datasets. If more than 4 months were undefined then the annual mean was not calculated. Much of the data north of 61° N was undefined in the derived dataset from 1883-1949 and 1966-1978.

The annual time series were plotted for the 16 grid points along with a low-pass filter and the linear trend. The linear trends of the derived wind speeds were found to be increasing with time at grid points 3, 6, 9, 10, 12, 13. Grid points 1, 2, 8 and 14 remained relatively constant and grid points 4, 5, 7 and 11 were decreasing with time (grid points 15 and 16 had insufficient data to reliably calculate a trend).

The NCEP/NCAR linear trend was increasing with time at all locations except grid point 2 which remained relatively constant. The NCEP/NCAR dataset is less than half the length of the derived dataset so this trend is less meaningful.

Figure 12 shows plots of 10 m wind speed at grid points 1 and 12. The low-pass filter demonstrates that significant variability exists in the long-term trend on an interdecadal time-scale.

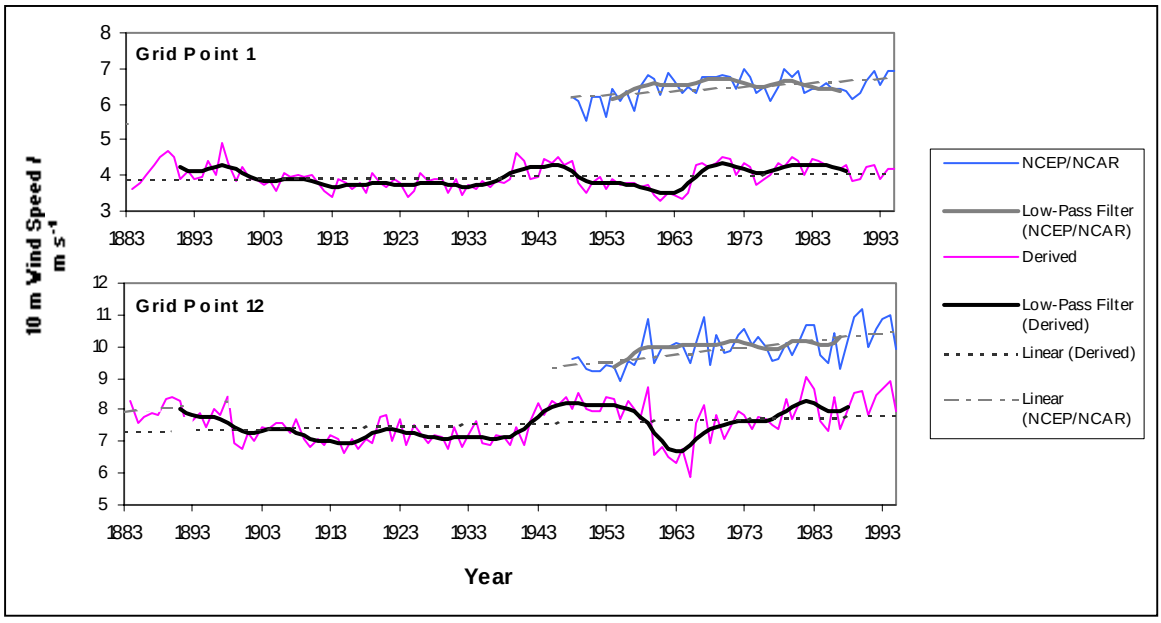

Figure 12. Time series plots showing derived and NCEP/NCAR 10 m wind speeds at grid points 1 and 12.

3.6 CORRECTING ERRORS IN THE UKMO MSLP DATASET

The homogeneity in the UKMO MSLP data has been discussed by Jones (1987). Daily observation times varied from 00:00hr to 12:00hr as shown in table 5.

Table 5. Observation times for each time period in the UKMO dataset [Source: Jones, 1987].

Time period (year(month))	Time of day of charts from which pressure data was extracted
1882(9) – 1898(12)	00:00hr
1899(1) – 1939(12)	12:00hr
1940(1) – 1948(12)	00:00hr
1949(1) – 1965(12)	12:00hr
1966(1) – 1995(12)	00:00hr

This inconsistency has led authors to apply corrections to wind speeds derived from the UKMO MSLP data. Palutikof *et al* (1992) used the Lamb Catalogue of weather types to derive regression equations related to the geostrophic winds. These were used over individual sites on land to calculate appropriate correction factors for the periods extracted from midday charts. Jenkinson & Collison (1977) also corrected their North Sea Gale Index for the same periods. Both sets of authors believe that the 1960-65 period contains pressure data that has been over-smoothed, probably due to interpolation methods used by early computers.

3.6.1 THE 1960-65 PERIOD

The over-smoothing in the early 1960s UKMO MSLP data is noticeable as a trough in the wind speed curve at all except one grid point. This feature appears to be an artefact of the UKMO dataset as it is not apparent in any NCEP/NCAR time series.

The NCEP/NCAR data can be used to correct the erroneous period in the derived dataset. The chosen correction method assumes that the year-to-year variation from 1960-65 is inaccurate in the derived wind speeds because they are calculated from an incorrect pressure gradient. Therefore the variability about the long-term NCEP/NCAR mean is superimposed onto the derived long-term mean as described by equation (4.1). All wind speeds used in these corrections are at a 10 m height.

$$der_t = \overline{der} + [NC_t - \overline{NC}] \qquad (4.1)$$

Where der_t is the derived wind speed at time step *t* and $\overline{der}$ is the mean wind speed. NC denotes the NCEP/NCAR wind speeds.

The correlation between the derived and the NCEP/NCAR wind speeds varies considerably over time and space. It would therefore not be justifiable to correct the time series at all grid points regardless of the relationship between the two datasets. R^2 values are shown in table 6 for 1948-95 annual mean wind speeds. They are generally low but the early 1960s period has a significant effect on the correlations as shown by the R^2 values listed from 1968-95. Figure 12 shows both datasets at grid point 12 exhibit similar curves apart from during the early 1960s. The 1948-95 R^2 value is 0.20

but the 1968-95 correlation rises to 0.75. Correlations between 15-year low-pass filtered means were also examined but were predominantly lower than those obtained from annual means.

Table 6. Correlations between the NCEP/NCAR and derived annual wind speeds at grid points 1-16.

Grid point / R^2	1	2	3	4	5	6	7	8	9	10	11	12	13	14	15	16
1948-1995	0.21	0.13	n.s.*	0.21	0.19	0.28	n.s.	0.23	0.47	0.24	0.10	0.20	0.29	0.15	0.25	0.25
1968-1995	0.32	0.19	0.19	0.28	0.76	0.40	0.33	0.72	0.72	0.70	0.63	0.75	0.74	0.16	0.65	0.84
Corrected 1948-1995	-	-	-	-	0.28	-	-	0.63	0.68	0.34	-	0.72	0.61	-	-	-

*n.s. denotes not significant at the 95% confidence level.

All grid points for which the R^2 values are greater than 0.70 for the period of 1968-95 are considered suitably correlated to apply corrections from the NCEP/NCAR data. Grid points 5, 8, 9, 10, 12 and 13 were chosen on this criteria. Grid point 16 was not corrected because data was missing from 1966-79. This process increased the 1948-95 correlation coefficients at all 6 sites but to varying extents (listed in table 6). The lowest R^2 value was obtained at grid point 5 which improved from 0.19 to 0.28 whilst a correlation of 0.68 was achieved at grid point 9.

3.6.2 THE 1899-39 PERIOD

Further examination of the time series revealed that half of the grid points exhibited lower than average wind speeds during the first half of the 20th century. This coincides with the 1899-1939 period when MSLP data was obtained from midday instead of midnight charts. The effect of this may be to slightly suppress calculated wind speeds which are often faster at night over the sea (Barthelmie *et al*, 1996). Since NCEP/NCAR data does not cover this period alternative methods are investigated.

Two approaches were adopted, both using NCEP/NCAR data to derive a ratio for the mean nightly wind speed to the mean daily wind speed. Firstly, 6-hourly MSLP data was obtained for 4 randomly chosen years (1972, 1980, 1985 and 1993) and the 80 m wind speeds were calculated. The mean midnight and midday means for the grouped years revealed that the winds were generally stronger in the day over most of the ocean a small margin (less than 5%). This method would lead to periods of low wind being reduced further, thus increasing the variability. Computing time restricted the number of years that could be used in with this approach.

The second approach used 6-hourly NCEP/NCAR surface winds at individual grid points for the entire 1948-95 period. The grid resolution of 2.5° x 2.5° limited data extraction to grid point 12. The closest available locations were used for 3 other grid points. At grid points 5 and 12 the midnight wind speeds were 2.5% and 0.7% greater than those at midday. However, grid points 9 and 13 exhibited higher midday wind speeds by 2.0% and 3.9% respectively. These correction factors are discussed further on page ***.

4. DISCUSSION

The validity of the method is discussed in light of the results. Relationships between the two wind speed datasets are considered along with long-term trends and NAO correlations. 80 m wind speeds are presented at certain grid points and are related to the economics of wind power generation.

4.1 VALIDITY OF THE METHOD

The method adopted here to calculate winds over open oceans involves a number of simplifications. The first assumption is that the pressure field can be accurately interpolated and used to derive wind speeds. Work by Palutikof *et al* (1992) and Palutikof and Holt (2000) supports this method. The assumption that MSLP data can be used to calculate a geostrophic wind only strictly applies when the isobars are straight and parallel, otherwise effects of centripetal acceleration and baroclinicity are relevant (Barry & Chorley, 1998). Despite these factors, the method has been used elsewhere and the errors are considered to be minor.

The conversion of the geostrophic to the near surface wind does not take account of processes within the boundary layer. Stability can have a significant effect on the wind speed profile (Stull, 1988). Incorporating this would require temperature profile data over the entire grid that is not available. The interaction between wind and waves has not been included, Troen and Petersen (1989) found this did not significantly affect the results. Furthermore, in this study the wind speeds of interest are 80 m above sea level, a height at which wind-wave characteristics are less pronounced than at the surface.

The corrections used for the 1960-65 period improve the homogeneity of the dataset and are justifiable with respect to the literature. The correction factors calculated for 1899-1939 were found to be both positive and negative but all less than 4% in magnitude. Since they are relatively small and the correction method is experimental the corrections for 1899-1939 have not been included in the final time series.

4.2 DERIVED AND NCEP/NCAR WIND SPEEDS

The results show that there are differences between the derived and the NCEP/NCAR wind speeds but the large-scale trends are similar. The higher winds in the NCEP/NCAR data are not spatially or temporally consistent so there is no evidence of a constant error. However, Stoffelen (1998) believes there to be a positive bias of approximately 6% in the NCEP/NCAR Reanalysis winds, subtracting this would bring the datasets closer in value. Both derived and NCEP/NCAR wind speeds are broadly accurate but fail to account for small-scale spatial variability. An example of this is the cyclogenesis in the Gulf of Genoa which is not discernible in the long-term mean plot. The EWA

(Troen & Petersen, 1989) was able to model this feature but their method included the effects of land, temperature and used a number of wind observations. Since the method used to derive wind speeds here is uniform over time, the failure to model sub-grid scale processes should not greatly influence long-term variability.

The greatest confidence should be placed in results over the open ocean, in the north-west of the domain where the highest correlation exists. Storm tracks and low pressure systems are known to cause high winds in the North Atlantic, this characteristic has been successfully modelled by the method used. However, above 61° N over half of the data is missing so results in this region should be interpreted cautiously.

The two datasets correlate poorly for about half of the Mediterranean Sea. The NCEP/NCAR wind speeds are partly derived from well-defined surface observations (Kalnay *et al*, 1996). They are sensitive to thermal, topographical, and coastal effects and are therefore more likely to be reliable in coastal and small sea regions than the derived winds. The lower wind speeds in the Mediterranean also increase the possible margin for error when examining variability. The temperature regime in the Mediterranean is likely to significantly affect the atmospheric stability, which is important in defining the surface wind speeds (Watson *et al*, 1999).

4.3 LONG-TERM TRENDS

The underlying long-term linear trend differed significantly between the two datasets at most grid points. Almost all NCEP/NCAR winds showed an increase in mean annual speed wind with time but these are obtained from only 57 years of data. Kalnay *et al* (1996) state that the NCEP/NCAR dataset cannot be considered uniformly reliable over time and space because of a biased spread of observations. Therefore, inaccuracies may exist for which it is hard to assess the degree of error. The 113 years of derived wind speeds showed both upward, stable and downward trends at different grid points. It is possible that the NCEP/NCAR model has identified a trend related to recent climatic changes. Investigating such an effect is beyond the scope of this study.

The 15-year low-pass filter at grid points in the north of the domain generally show a trough in wind speed in the early 20th century and a rising trend in the latter part. Decadal means reflect this trend at most North Atlantic grid points where wind speeds were generally lower in the first half of the 20th century with a significant upturn around 1950. The linear trend in the two datasets may in fact be similar but the NCEP/NCAR winds do not date back far enough to detect the decline in speeds in the early 1900s. The increase in the late 20th century is visible at 10 of the 16 grid points in the derived data.

4.4 SPATIAL CORRELATION BETWEEN GRID POINTS

The spatial correlation between grid points was examined including the corrected wind speeds. Table 7 shows the results in a correlation matrix.

Table 7. Correlation matrix showing R^2 values between decadal mean wind speeds at grid points 1-16.

GRID POINTS	1	2	3	4	5	6	7	8	9	10	11	12	13	14	15
1	-														
2	0.11	-													
3	0.38	**0.7**	-												
4	0.13	NEG	NEG	-											
5	NEG*	NEG	NEG	0.50	-										
6	**0.71**	0.27	0.69	0.02	NEG	-									
7	0.02	NEG	NEG	0.55	0.36	0.02	-								
8	0.19	0.54	0.51	NEG	NEG	0.34	NEG	-							
9	0.55	0.13	0.49	NEG	NEG	0.49	NEG	0.35	-						
10	0.47	0.18	0.48	NEG	NEG	0.42	NEG	0.51	**0.75**	-					
11	0.51	0.02	0.21	0.02	NEG	0.43	0.06	0.06	0.58	0.26	-				
12	0.14	0.24	0.36	NEG	NEG	0.16	NEG	0.52	0.46	**0.80**	0.06	-			
13	0.17	0.35	0.52	NEG	NEG	0.26	NEG	0.58	0.61	**0.75**	0.18	**0.89**	-		
14	0.16	0.16	0.26	NEG	NEG	0.18	NEG	0.22	0.52	0.32	0.63	0.32	0.54	-	
15**	0.40	**0.79**	0.68	NEG	NEG	0.52	NEG	0.62	0.69	0.65	0.45	0.08	0.42	0.28	-
16**	0.23	**0.91**	0.64	NEG	NEG	0.31	NEG	**0.74**	**0.92**	**0.86**	0.69	0.34	**0.72**	**0.78**	0.64

*NEG denotes that a negative correlation was found.
** The correlations with grid points 15 and 16 are of little use because about half of the data is missing.

If an R^2 value of 0.5 is used to denote significance then there is no spatially coherent pattern of correlation. R^2 values above 0.7 (shown in bold in table 7) reveal that the only significant cluster of similar trends is found to the north of the UK between grid points 10, 12 and 13. There is also a strong correlation between grid points 11 and 14 in the Baltic (0.63). The Mediterranean shows less significant grouping with the highest correlation between grid points 4 and 5 (0.50).

4.5 RELATING THE NAO TO SURFACE WINDS

The NAO explains a similar degree of the variance in both the NCEP/NCAR and derived datasets. Exposed sites receive more westerly flow when the NAO is high because the pressure gradient is larger between the Icelandic Low and the Azores High (Hurrell, 1995). It is therefore unsurprising that the highest correlation with the NAO exists in the North Atlantic. At grid point 10 the variation in the NAO explains 62% of the winter wind speed variation but the relationship is much weaker in the Mediterranean where temperature regimes have a more pronounced effect on winds.

The Intergovernmental Panel on Climate Change (Watson *et al*, 1996) describes the link between positive trends in NAO index during the 1920s and 1930s and the intensified westerly winds in the

extratropical Northern Hemisphere. This trend is not apparent in the derived wind speeds with no significant peaks during these decades except at grid point 2.

The running correlation was extended for comparison with the NCEP/NCAR winds to include the most recent data (1996-1999) and this showed a downward trend in the last three years calculated. The NAO index oscillated to an extreme negative value in 1996 so this may explain the lower correlations in recent years. It is likely that the correlation between the derived wind speeds and the NAO would also exhibit this trend if MSLP data was available for this period.

4.6 LONG-TERM VARIABILITY

Figure 13 is a contour plot of the lower 95% confidence interval of the long-term mean 80 m wind speed. This is useful because it combines the average with a measure of the variability. Hence the blue areas exhibit the highest wind speeds taking into account the long-term variability. The region above 61°N includes much missing data so the confidence interval is less accurate. Note that the plot does not include the corrections made from 1960-65 at some grid points so there is a small degree of uncertainty in the values. Waters around the UK represent the sites of highest potential for wind power generation based on wind speeds alone.

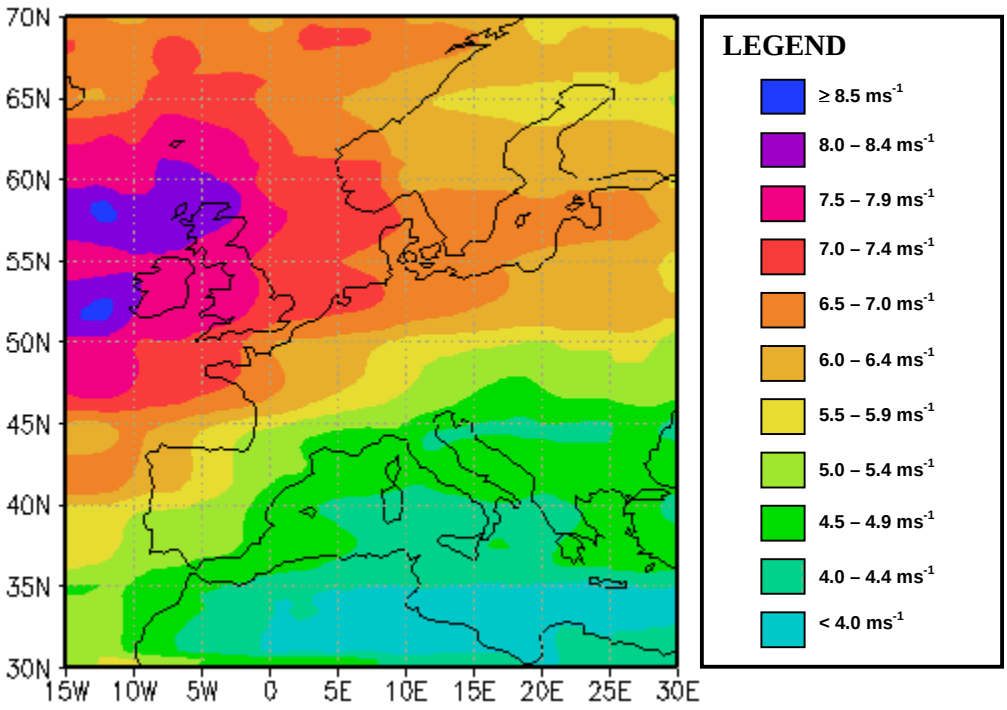

Figure 13. Lower 95% confidence limits for mean annual 80 m wind speeds.

Time series are presented in figure 14 for grid points in the Northern Atlantic region (12), Southern Atlantic region (2), Baltic Sea (14) and the Mediterranean (5). The annual mean wind speeds are

presented with upper and lower confidence levels. Grid points 5 and 12 have been corrected from 1960-65. There appears to be some persistence in the wind speeds on a decadal scale. For example, at grid point 12 winds fall below the long-term mean for much of the early 19th century.

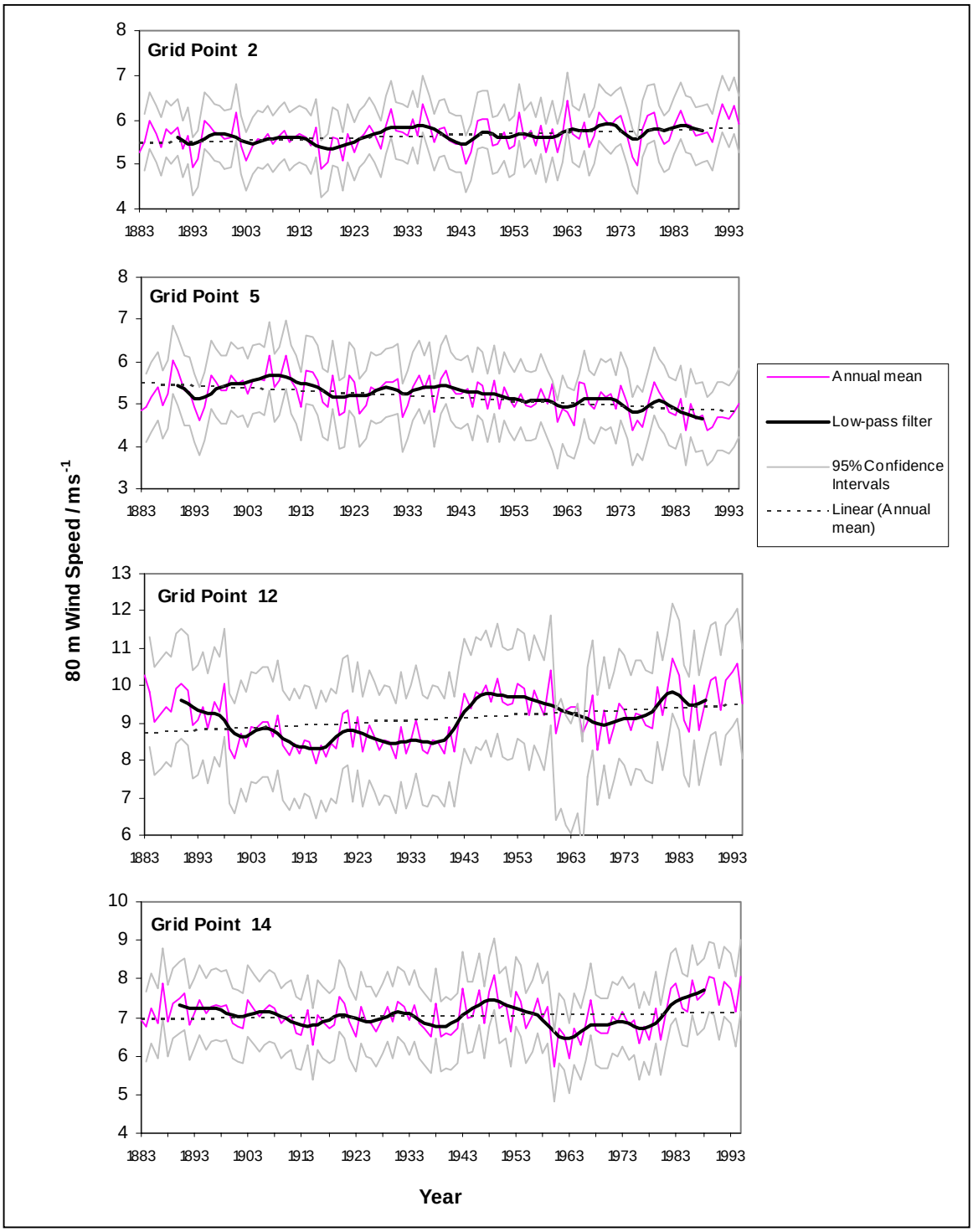

Figure 14. Annual mean 80 m wind speeds at grid points 2, 5, 12 and 14. The 95% confidence intervals are defined as 2 standard deviations from the mean as recommended by Wilks (1995).

4.7 RELATING MEAN WIND SPEEDS TO POWER OUTPUT AND ECONOMIC IMPLICATIONS FOR OFFSHORE WIND ENERGY

In the last 15 years the cost of wind power has been steadily decreasing and further cost reductions are likely due to improved technology, design and larger scale projects (European Commission, 1999). A typical modern Danish 600 kW turbine will recover its energy costs of manufacture, maintenance and scrapping in only 3 months (Danish Wind Turbine Manufacturers Association, 1997). The most important factor regarding the economics of wind power is the wind resource itself.

The EWA (Troen & Petersen, 1989) describes a simple method for estimating energy production from the mean wind speed. This takes into account the size of the wind turbine (using swept area) and the roughness class of the surface. Their method is used here for a hub height of 80 m and a rotor radius of 40 m (as suggested by Jamieson and Quarton (1999) for future offshore developments). Equation (4.1) uses a cubic relationship between the mean wind speed and the power density:

$$\text{Power density (W m}^{-2}) = -2.682\text{MWS}^3 + 75.964\text{MWS}^2 - 453.37\ \text{MWS} + 775.31 \quad \text{(Eq. 4.1)}$$

Where MWS is the mean wind speed in ms^{-1}.

The resulting power density is corrected to an 80 m height (using a conversion factor given in the EWA as 2.05) and multiplied by the swept area (5027 m^2) to obtain the available power in kW. This is then converted to an annual estimate (in GWh). In practice, only about 25% of the available power is converted to energy (Troen & Petersen, 1989) so the annual estimate is divided by 4 to give the estimated energy production.

Figure 15 shows the mean energy production calculated from decadal mean wind speeds at grid point 12 in the North Atlantic. This grid point was chosen because the 1960-65 period has been corrected and is located in a region of high wind speed variability. The decadal mean energy production varies between 17.2 and 25.3 GWh yr^{-1}. The largest percentage change between successive decades is from 1936-45 to 1946-55 (+26.3%). Such a change would have a significant effect on wind energy generation. Both decades include data derived from midday and midnight pressure charts so this variability is unlikely to be the result of inhomogeneities.

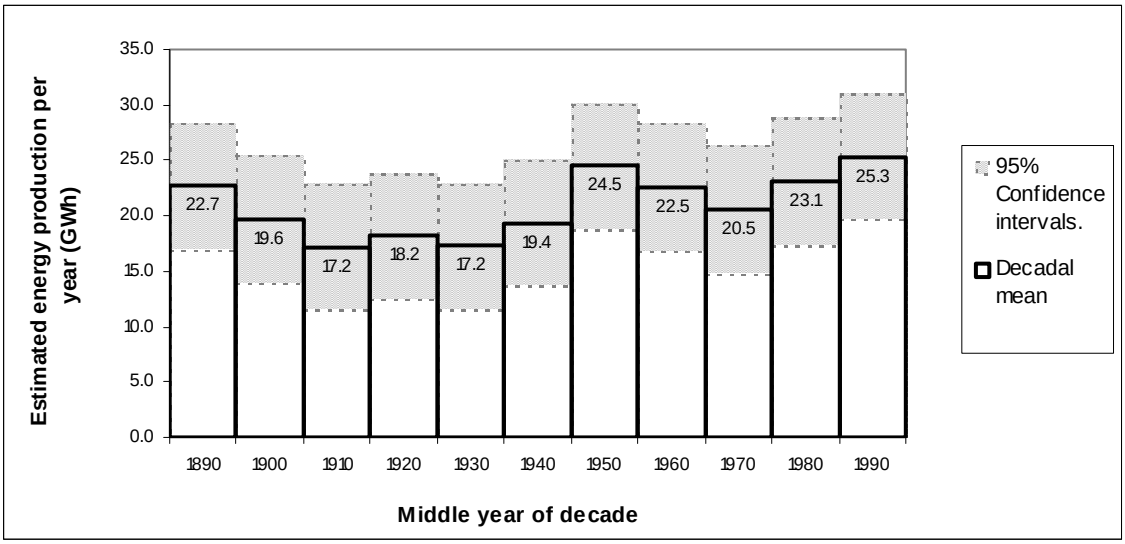

Figure 15. Estimated decadal mean energy production from a wind turbine at grid point 12 from 1886-1995.

The estimated energy generated from other grid points showed that interdecadal variation is an important factor when considering the economics and siting of offshore wind turbines. Grid point 5 in the Mediterranean was also examined. The low mean and high variability led to a decrease of 39.6% from 1906-15 (3.41 GWh yr^{-1}) to 1916-25 (2.06 GWh yr^{-1}).

5. CONCLUSIONS

5.1 LONG-TERM VARIABILITY IN OFFSHORE WIND SPEEDS

The creation and analysis of a long-term wind speed dataset has shown that interdecadal variability can be large enough to affect power generation from offshore wind turbines at some locations. This supports the hypothesis stated in the introduction that, as on land, long-term variability over European waters may affect the economics of the siting of wind turbines.

The mean 80 m wind speeds can vary by as much as 0.9 ms^{-1} between decades. Variation in energy production is estimated to alter by up to 40% at a low wind speed site and 26% at a high wind speed site.

Comparisons with literature confirm the validity of the method and results are close to observations (maximum error of 17%). NCEP/NCAR data shows general trends similar to those derived here. Neither dataset is believed to be entirely accurate but both can be used to examine long-term variability.

At locations where the NCEP/NCAR data closely matches the derived winds it is possible to correct an anomalous period in the latter. However, this must be performed at each grid point and not applied to the entire dataset.

The NAO index can be used to describe approximately half of the variability in the mean winter wind speeds above oceans around the UK and the Baltic Sea. This relationship falls off over the Mediterranean where it is not useful.

This work can be considered as a useful addition to the POWER project which will provide the wind industry with important information about offshore wind fields. Preliminary identification of suitable areas for siting wind turbines would be followed by in-situ measurements. Increasing the understanding of long-term trends in offshore winds will reduce uncertainties and make offshore wind energy generation more viable in the EU. The future expansion of the wind energy market is likely to play a significant part in reducing greenhouse gas emissions.

5.2 SUGGESTIONS FOR FURTHER WORK

Suggestions for further research following this study are:

1. A more complex model including coastal effects such as the POWER project's Coastal Discontinuity Model would improve the applicability of this technique.

2. The geostrophic drag relationship (described on page ***) could be solved by iteration to calculate more accurate values for the surface roughness and friction velocity. Lange & Højstrup (1999) have developed a more complex model that improves the description of this relationship in shallow coastal waters.

3. The inclusion of atmospheric stability in the model would improve the reliability of the wind speeds calculated by this method.

4. The method used to adjust the derived dataset using the NCEP/NCAR 1960-65 wind speeds could be used to modify the data over the entire domain. A computer programme could be written to read the monthly mean wind speeds from both data files, calculating the R^2 value from 1968-95 at each grid point and then applying the correction where the correlation coefficient exceeds 0.70.

5. A suitable method of correcting the 1899-1939 and 1949-59 periods would improve the long-term homogeneity of the dataset. Comparing NCEP/NCAR mean surface winds at 00:00hr and 12:00hr from 1948-95 is the most promising method.

REFERENCES

Ahrens, C.D. (1994). *Meteorology Today* (5th Ed.). West Publishing, Minneapolis, USA.

Barry, R.G. & Chorley, R.J. (1998). *Atmosphere, Weather & Climate* (7th Ed.). Routledge, London, UK.

Barthelmie, R.J. (1991). *Predicting on- and off-shore wind speeds for wind energy applications.* Ph.D. Thesis. University of East Anglia, Norwich, UK.

Barthelmie, R.J. (1993). *Prospects for offshore wind energy: The state of the art and future opportunities.* British Wind Energy Association, Department of Trade and Industry and Wind Engineering Seminar.

Barthelmie, R.J. (1997). Evaluation of empirical and statistical methods for predicting offshore wind speeds. *Wind Engineering*. **21**: (2), 102-112.

Barthelmie, R.J., Grisogono, B. & Pryor, S.C. (1996). Observations and simulations of diurnal cycles of near-surface wind speeds over land and sea. *Journal Geophys.Res.- Atmospheres.* **101**: (D16), 21327-21337.

Barthelmie, R.J., Palutikof, J.P. & Davies, T.D. (1991). Predicting UK offshore wind speeds. *Annales Geophysicae – Atmospheres, Hydrospheres and Space Sciences,* **9**: (11), 708-715.

Border Wind. (1998). *Offshore Wind Energy. Building a New Industry in Britain.* A Report for Greenpeace by Border Wind.

Børresen, J.A. (1987). *Wind Atlas for the North Sea and the Norwegian Sea.* Norwegian University of Press, Oslo, Norway.

BWEA. (2000). Frequently asked questions [www]. The British Wind Energy Association web site. http://www.bwea.com/primer/faq.html (Accessed: 25th May 2000).

Carretero, J.C., Gomez, M., Lozano, I., de Elvira, A.R., Serrano, O., Iden, K., Reistad, M., Reichardt, H., Kharin, V., Stolley, M., von Storch, H., Gunther, H., Pfizenmayer, A., Rosethal, W., Stawarz, M., Schmith, T., Kaas, E., Li, T., Alexandersson, H., Beersma, J., Bouws, E., Komen, G., Rider, K., Flather, R., Smith, J., Bijl, W., de Ronde, J., Mietus, M., Bauer, E., Schmidt, H., Langenberg, H. (1998). Changing waves and storms in the northeast Atlantic? *Bulletin of the American Meteorological Society*. **79**: (5), 741-760.

CDC. (2000). NCEP/NCAR Reanalysis Problems List [www]. Climate Diagnostics Center web site. http://www.cdc.noaa.gov/cdc/reanalysis/problems.shtml (Accessed: 30th June 2000).

CRU. (2000). Climatic Research Unit web site [www]. NAO description site with links to download the NAO index dataset 1821-1997. http://www.cru.uea.ac.uk/cru/data/nao.htm (Accessed: 10th May 2000).

Danish Wind Turbine Manufacturers Association. (1997). *Wind Power Information Note*. 16 November 1997. DWTMA.

DETR. (1998). *UK Climate Change Programme. Consultation Paper*. Department of the Environment, Transport and the Regions.

ENDS. (2000). Environment Daily European environmental news and archive service [www]. Environmental Data Services Ltd. http://www.ends.co.uk/envdaily/ (Accessed: 10th May 2000).

European Commission. (1999). *Wind Energy in Europe – The Facts*. EC Directorate-General for Energy.

Fiorino, M. (1995). REGRID, Version 2.0beta. On-line user manual [www]. http://dao.gsfc.nasa.gov/software/grads/lats4d/regrid2.doc (Accessed: 14th April 2000).

Haber, A. & Runyon, R.P. (1973). *General Statistics* (2nd Ed.). Addison-Wesley Publishing Company, London, UK.

Hooper, D. (2000). Electronic-mail correspondence regarding the NCEP/NCAR wind speed averaging method. Climate Diagnostics Center. (Received: 28th June 2000).

Hsu, S.A. (1988). *Coastal Meteorology*. Academic Press Inc., San Diego, USA.

Hurrell, J.W. (1995). Decadal trends in the North-Atlantic Oscillation - Regional temperatures and precipitation. *Science*. **269**, 676-679.

Jamieson, P. & Quarton, D.C. (1999). Technology development for offshore. *Proceedings of the 1999 European Wind Energy Conference*. 1-5 March 1999, Nice, France, 289-293.

Jenkinson, A.F. & Collison, F.P. (1977). *An initial climatology of gales over the North Sea.* Met. Office. 13 Branch Memorandum 62. UK Met. Office, Bracknell, UK.

Jones, P.D. (1987). The early twentieth century Arctic high – fact or fiction? *Climate Dynamics*. **1**, 63-75.

Jones, P.D., Jonsson, T. & Wheeler, D. (1997). Extension to the North Atlantic Oscillation using early instrumental pressure observations from Gibraltar and south-west Iceland. *International Journal of Climatology*. **17**: (13), 1433-1450.

Kalnay, E., Kanamitsu, M., Kistler, R., Collins, W., Deaven, D., Gandin, L., Iredell, M., Saha, S., White, G., Woollen, J., Zhu, Y., Chelliah, M., Ebisuzaki, W., Higgins, W., Janowiak, J., Mo, K.C., Ropelewski, C., Wang, J., Leetmaa, A., Reynolds, R., Jenne, R. & Joseph, D. (1996). The NCEP/NCAR 40-year Reanalysis Project. *Bulletin of the American Meteorological Society*. **77**: (3), 437-471.

Kidder, S.Q. & Vonder Haar, T.H. (1995). *Satellite Meteorology. An Introduction.* Chapter 7: Winds, 233-258. Academic Press Inc., San Diego, USA.

Kotz, S. & Johnson, N.L. (Eds.). (1985). *Encyclopaedia of Statistical Science. Volume 3.* John Wiley & Sons, New York, USA.

Lange, B. & Højstrup, J. (1999). The influence of waves on the offshore wind resource. *Proceedings of the 1999 European Wind Energy Conference*, 1-5 March 1999, Nice, France, 1216-1219.

Matthies, H., Garrad, A. D., Adams, B.M., Scherweit, M., & Siebers, M. (1994). An Assessment of the Offshore Wind Potential in the EC. *Proceedings of the 14th European Wind Energy Conference 1994.* 111-115.

Mehta, V.M., Suarez, M.J., Manganello, J.V. & Delworth, T.L. (2000). Oceanic influence on the North Atlantic Oscillation and associated Northern Hemisphere climate variations: 1959-1993. *Geophysical Research Letters.* **27**, 121-124.

Moore, D.J. (1982). 10 to 100 m winds calculated from 900 mb wind data. *Proceedings of the 4th British Wind Energy Association Workshop*. 197-205. BHRA Fluid Engineering, Cranfield, UK.

Osborn, T.J., Briffa, K.R., Tett, S.F.B., Jones, P.D. & Trigo, R.M. (1999). Evaluation of the North Atlantic Oscillation as simulated by a coupled climate model. *Climate Dynamics*. **15**, 685-702.

Paeth, H., Hense, A., Glowienka-Hense, R., Voss, R. & Cubasch, U. (1999). The North Atlantic Oscillation as an indicator for greenhouse-gas induced regional climate change. *Climate Dynamics*. **15**, 953-960.

Palutikof, J.P., Guo, X. & Halliday, J.A. (1992). Climate variability and the UK wind resource. *Journal of Wind Engineering and Industrial Aerodynamics*. **39**, 243-249.

Palutikof, J.P., Holt, T. & Skellern, A. (1997). Wind: Resource and Hazard. **In:** *Climates of the British Isles. Present, past and future.* Eds. M. Hulme & E. Barrow, 220-242. Routledge, London/New York.

Palutikof, J.P. & Holt, T. (2000). Synoptic-scale wind data suitable for the preliminary assessment of the off-shore wind resource. *Proceedings of the Euro Seminar: Offshore Wind Energy in Mediterranean and other European Seas: Technology and potential applications*. 13-15 April 2000, Sicilia, Italy, 93-107.

Palutikof, J.P., Kelly, P.M., Davies, T.D. & Halliday, J.A. (1987). Impacts of spatial and temporal wind speed variability on wind energy output. *J.Climate Appl. Meteorol.* **26**, 1124-1133.

Poulos, S.E., Drakopoulos, P.G. & Collins, M.B. (1997). Seasonal variability in sea surface oceanographic conditions in the Aegean Sea (Eastern Mediterranean): an overview. *Journal of Marine Systems*. **13,** 225-244.

Press, W.H., Teukolsky, S.A., Vetterling, W.T. & Flannery, B.P. (1997). *Numerical Recipes in Fortran 77. The Art of Scientific Computing* (2nd Ed.). Cambridge University Press, Cambridge, UK.

Rodwell, M.J., Rowell, D.P. & Folland, C.K. (1999). Oceanic forcing of the wintertime North Atlantic Oscillation and European climate**.** ***Nature***. **398**, 320-323.

Seinfeld, J.H. & Pandis, S.N. (1998). *Atmospheric Chemistry and Physics. From Air Pollution to Climate Change*. John Wiley and Sons Inc., New York, USA.

Serway, R.A. (1996). *Physics for Scientists and Engineers* (4th Ed.). Saunders College Publishing, Philadelphia, USA.

Stationary Office. (1997). *Digest of United Kingdom Energy Statistics.* Stationary Office, London, UK.

Stephenson, D.B., Pavan, V. & Bojariu, R. (2000). Is the North Atlantic Oscillation a random walk? *International Journal of Climatology*. **20**: (1), 1-18.

Stoffelen, A. (1998). Toward the true near-surface wind speed: Error modeling and calibration using triple collocation. *Journal Geophys.Res.- Oceans.* **103**: (C4), 7755-7766.

Stull, R.B. (1988). *An Introduction to Boundary Layer Meteorology*. Kluwer Academic Publishers, Dordrecht, The Netherlands.

Troen, I. & Petersen, E.L. (1989). *European Wind Atlas*. Risø National Laboratory, Roskilde, Denmark.

Uppenbrink, J. (1999). Climate variability - The North Atlantic oscillation. *Science.* **283**, 948-949.

Ward, M.N. & Hoskins, B.J. (1996). Near-surface wind over the Global Ocean 1949-1988. *Journal of Climate*. **9**: (8), 1877-1895.

Watson, G.M., Halliday, J.A., Palutikof, J.P., Holt, T., Barthelmie, R.J., Coelingh, J.P., Folkerts, L., Van Zuylen & E.J., Cleijne, J.W. (1999). POWER – A Methodology for Predicting Offshore Wind Energy Resources. *Proceedings of the 1999 European Wind Energy Conference*, 1-5 March 1999, Nice, France, 1105-1108.

Watson, R.T., Zinyonera, M.C. & Moss, R.H. (Eds.). (1996). *Climate Change 1995: Report on impacts, adaptation and mitigation of Climate Change*. Working Group II, Intergovernmental Panel on Climate Change. Cambridge University Press, Cambridge, UK.

White, P.A. (1985). The offshore wind energy resource around the United Kingdom. *Wind Engineering*. **9**: (4), 221-233.

Wilks, D.S. (1995). *Statistical Methods in the Atmospheric Sciences*. Academic Press, San Diego, USA.

Woodruff, S.D., Diaz1, H.F., Elms, J.D., and Worley, S.J. (1998). COADS Release 2 Data and Metadata Enhancements for Improvements of Marine Surface Flux Fields. *Phys. Chem. Earth*. **23**: (5-6), 517-526.

Wu, J. (1995). Sea-surface winds – A critical input to oceanic models, but are they accurately measured. *Bulletin of the American Meteorological Society*. **76**: (1), 13-19.

ACKNOWLEDGEMENTS

I would like to thank my supervisor Jean Palutikof for all her expert guidance, help and critical thinking. Thanks also to Tom Holt for showing me where and how to obtain the data and David Lister for putting up with my presence in his tiny office for two months.

Thank you to Don Hooper (of the Climate Diagnostics Center) for answering my e-mails with haste and putting me back on track.

APPENDIX 1: List of Abbreviations

BWEA	British Wind Energy Association
CDC	Climate Diagnostics Center
CDM	Coastal Discontinuity Model
CRU	Climatic Research Unit (University of East Anglia)
ENSO	El Niño Southern Oscillation
EU	European Union
EWA	European Wind Atlas
G^{r}ADS	Grid Analysis and Display System
GWh	Gigawatt hour
hPa	hectoPascals
kW	Kilowatt
m.s.l.	mean sea level
MSLP	mean sea level pressure
MWS	mean wind speed
NAO	North Atlantic Oscillation
NCAR	National Center for Atmospheric Research (US)
NCEP	National Centers for Environmental Prediction (US)
POWER	Predicting Offshore Wind Energy Resource Project
SLP	sea level pressure
TWh yr^{-1}	Terrawatt hours per year
UEA	University of East Anglia
UKMO	United Kingdom Meteorological Office
WASA	Wave And Storm in the North Atlantic Project
WA^{S}P	Wind Atlas Analysis and Application Programme

APPENDIX 2: Fortran 77 Programme to Read the MSLP Grid and Calculate Wind Speeds

```
       PROGRAM PRESWIND
C
C  THIS PROGRAMME READS A MEAN SEA LEVEL PRESSURE GRID AT EACH
C  TIMESTEP FROM AN INPUT FILE OF 4 YEARS.  IT THEN USES THE MSLPs AT 2
DEG
C  LONGITUDE AND 1 DEG LATITUDE TO EACH GRIDPOINT TO CALCULATE THE
PRESSURE
C  DIFFERENCE AND THEN THE GEOSTROPHIC WIND.
C  REGRESSION EQUATIONS ARE USED TO THEN CALCULATE THE FRICTION WIND
C  AND FINALLY THIS IS CONVERTED TO THE 80 METRE WIND (OR CHOSEN HEIGHT).
C
C  NOTE THAT THE OUTPUT FILE IS TWO COLUMNS AND TWO ROWS SMALLER
C  THAN THE INPUT FILE.
C
C  DEFINE USEFUL PARAMETERS: NO. OF ROWS AND COLUMNS, RECORD LENGTH OF
INPUT
C  AND OUTPUT FILES, PI, RADIUS OF EARTH,
C  DENSITY OF AIR, CIRCUMFERENCE OF EARTH (ON Y GRID), DISTANCE OF
PRESSURE
C  GRADIENT IN BOTH DIRECTIONS
C
       PARAMETER (NROWS=85, NCOLS=99, NDATA=NCOLS*NROWS)
       PARAMETER (MDATA=((NCOLS-8)*(NROWS-4)))
       PARAMETER (PI=3.141593, RA=6370000.0, DENS=1.225)
       PARAMETER (CIRY=2.0*PI*RA, DY=CIRY/180.0)
C
C
C  DEFINE ARRAYS: PRESSURE, INPUT DATA, OUTPUT DATA, 10 METRE WIND (WHICH
C  HAS A THIRD PART FOR THE U AND V WIND)
C
       REAL PR (NCOLS,NROWS), AINP(NDATA)
       REAL OUTW (MDATA), V80(NCOLS-8,NROWS-4,2)
C
C  PREPARE INPUT AND OUTPUT FILES
C
       OPEN (UNIT=1, FILE='ukmo/int/uk1991-95pr.dat', STATUS='old',
     * ACCESS='direct', RECL=NDATA)
       OPEN (UNIT=2, FILE='ukmo/80mwind/uk1991-95dy.dat',
     * STATUS='new', ACCESS='direct', RECL=MDATA)
       IREC=0
       IR=0
C
C  PRINT SOME OF THE PARAMETERS TO CHECK
C
       PRINT*,'PI ',PI,' RA ',RA,' DENS ',DENS,' CIRY ',CIRY,' DY ',DY
C
C  NO LEAP YEAR INVOLVED IF YEAR 1 IS 1900 THEREFORE NO. OF DAYS IS ONE
LESS
C
      PRINT*,'PLEASE ENTER THE START YEAR.'
      READ*,NYR
      IF(NYR.EQ.1900) THEN
      NDAYS=1460
```

```
      ELSE
      NDAYS=1461
      END IF
      PRINT*,'NUMBER OF DAYS IS ',NDAYS
C
C  BEGIN TIME-STEP LOOP
C
      DO 10 IT=1,NDAYS
      PRINT*,'TIME ',IT
      K=0
      IREC=IREC+1
C
C  SET UP LOOP TO READ SPATIAL GRID AT THIS TIME STEP
C
          READ (1,REC=IREC)(AINP(IQ),IQ=1,NDATA)
          M=0
          DO 20 IY=1,NROWS
            DO 15 IA=1,NCOLS
            M=M+1
            PR(IA,IY)=AINP(M)
 15         CONTINUE
 20       CONTINUE
C
C  CALCULATE GEOSTROPHIC WINDS AT THIS TIME STEP, NOTE THAT
C  BOUNDARY IS EXCLUDED FROM LOOP STEPS BECAUSE VALUES ONLY
C  NEEDED FOR CALCULATIONS WITHIN GRID
C
          DO 30 IY=3,NROWS-2
C
C  DEFINE LATITUDE (IN DEGREES AND RADIANS), CORIOLIS FORCE, CIRCUMFERENCE
AT
C  THIS LATITUDE AND DISTANCE SPANNING PRESSURE GRADIENT ON X GRID
C
          DLAT=(((FLOAT(IY))*0.5)+28.5)
          RLAT=(((FLOAT(IY))*0.5)+28.5)*PI/180.0
          CF=2.0*(7.27220522E-5)*(SIN(RLAT))
          RRAD=RA*(COS(RLAT))
          CIRX=2.0*PI*RRAD
          DX=CIRX/90.0
C
C  DEFINE THE CONSTANTS C1....C8 THAT ARE USED IN THE REGRESSION
C  EQUATIONS TO CALCULATE THE FRICTION WIND.  THESE VARY WITH LATITUDE
C  AND ARE SPLIT INTO 5 DEGREE BANDS.  HENCE THERE ARE 8 BANDS AND 8
C  EQUATIONS RELATING THE FRICTION VELOCITY AND THE GEOST. WIND.
C
            IF(DLAT.LT.30.0.OR.DLAT.GT.70.0) THEN
            PRINT*,'LATITUDE IS OUT OF RANGE AT: ',DLAT
            STOP
            ELSE
            END IF
            IF(DLAT.LE.35.0) THEN
            C1=0.02976101061
            C2=0.93046032708
            C3=0.02972359419
            C4=0.93795455445
            C5=0.02955486116
            C6=0.94147848276
            C7=0.02926028874
```

```
C8=0.94499933615
GO TO 25
ELSE
END IF
IF(DLAT.LE.40.0) THEN
C1=0.03001634142
C2=0.92992113232
C3=0.02998020698
C4=0.93750408829
C5=0.02980885037
C6=0.94107080548
C7=0.02950902905
C8=0.94463390825
GO TO 25
ELSE
END IF
IF(DLAT.LE.45.0) THEN
C1=0.03022109915
C2=0.92949036582
C3=0.03018603674
C4=0.93714392961
C5=0.03001257615
C6=0.94074487221
C7=0.02970852495
C8=0.94434181020
GO TO 25
ELSE
END IF
IF(DLAT.LE.50.0) THEN
C1=0.03039483610
C2=0.92912602404
C3=0.03036071399
C4=0.93683909664
C5=0.03018546845
C6=0.94046901342
C7=0.02987781415
C8=0.94409462570
GO TO 25
ELSE
END IF
IF(DLAT.LE.55.0) THEN
C1=0.03054196124
C2=0.92881834026
C3=0.03050865743
C4=0.93658150562
C5=0.03033190075
C6=0.94023590841
C7=0.03002118538
C8=0.94388577608
GO TO 25
ELSE
END IF
IF(DLAT.LE.60.0) THEN
C1=0.03066564530
C2=0.92856029190
C3=0.03063304502
C4=0.93636534783
C5=0.03045501837
```

```
            C6=0.94004029820
            C7=0.03014172276
            C8=0.94371053668
            GO TO 25
            ELSE
            END IF
            IF(DLAT.LE.65.0) THEN
            C1=0.03076355799
            C2=0.92835641381
            C3=0.03073152474
            C4=0.93619448453
            C5=0.03055249307
            C6=0.93988567615
            C7=0.03023715048
            C8=0.94357202735
            GO TO 25
            ELSE
            END IF
            IF(DLAT.LE.70.0) THEN
            C1=0.03085138766
            C2=0.92817383658
            C3=0.03081987065
            C4=0.93604140893
            C5=0.03063993773
            C6=0.93974714999
            C7=0.03032275571
            C8=0.94344794409
            GO TO 25
C
C  CHECK THAT LATITUDE HAS NOT VENTURED OUT OF RANGE
C
            ELSE
            PRINT*,'LATITUDE IS NOT IN RANGE AT: ',DLAT
            STOP
            END IF
C
C  START DO LOOP TO CALCULATE GEOSTROPHIC WINDS AT ALL GRID POINTS
C  ALONG THIS LINE OF LATITUDE. NOTE PX=PRESSURE CHANGE IN X-DIR,
C  VGX=GEOSTROPHIC WIND IN X-DIR (SAME NOTATION FOR Y)
C
 25          DO 40 IX=5,NCOLS-4
             PX=(PR(IX-4,IY)-PR(IX+4,IY))*100.0
             VGX=(-1.0/(DENS*CF))*(PX/DX)
             PY=(PR(IX,IY+2)-PR(IX,IY-2))*100.0
             VGY=(-1.0/(DENS*CF))*(PY/DY)
C
C  SET UP TWO-STEP LOOP TO CALCULATE X-DIRECTION THEN Y-DIRECTION WIND
C
               DO 55 IP=1,2
               IF (IP.EQ.2) THEN
               VG=VGY
               ELSE
               VG=VGX
               END IF
C
C  CONVERT THE GEOSTROPHIC WIND INTO THE FRICTION WIND (VF) USING ONE
C  OF SIX REGRESSION EQUATIONS DEPENDING ON VALUE OF VG.
C  IF ANY OF THE PRESSURES ARE UNDEFINED THEN MAKE THE 80m WIND UNDEFINED
```

```
C
            VG1=ABS(VG)
            IF(PR(IX-4,IY).EQ.-9999.000.OR.PR(IX+4,IY).EQ.-9999.000.
     *      OR.PR(IX,IY+2).EQ.-9999.000.OR.PR(IX,IY-2).EQ.-9999.000)
     *      THEN
            V80(IX-1,IY-1,IP)=-9999.000
            GO TO 55
            ELSE
            END IF
            IF(VG1.GT.100.0) THEN
            PRINT*,'TIME-STEP:  ',IT,'    GRID  X: ',IX,' Y: ',IY,
     *      '  HAS A VG OF ',VG,' m/s.'
            STOP
            ELSE
            END IF
            IF(VG1.GT.25.0) THEN
            VF=C7*(VG1**C8)
            GO TO 50
            ELSE
            END IF
            IF(VG1.GT.5.0) THEN
            VF=C5*(VG1**C6)
            GO TO 50
            ELSE
            END IF
            IF(VG1.GT.1.5) THEN
            VF=C3*(VG1**C4)
            GO TO 50
            ELSE
            END IF
            IF(VG1.GE.0.0) THEN
            VF=C1*(VG1**C2)
            GO TO 50
            ELSE
            PRINT*,'TIME: ',IT,' X: ',IX,' Y: ',IY
            PRINT*,'Vg IS NEGATIVE!!'
            STOP
            END IF
C
C  CALCULATE THE 80 METRE WIND FROM THE FRICTION WIND AND PUT INTO
C  1-D OUTPUT ARRAY AS THE NEXT ITEM OF DATA
C
 50         V80(IX-1,IY-1,IP)=(VF/0.4)*(LOG(80.0/0.0002))
 55         CONTINUE
            K=K+1
C
C  IF EITHER 80m WIND IS UNDEFINED THEN COMBINED 80 METRE WIND IS MADE
EQUAL
C  TO -9999.000 (UNDEFINED)
C
            IF(V80(IX-1,IY-1,1).EQ.-9999.000.OR.V80(IX-1,IY-1,2).
     *      EQ.-9999.000) THEN
            OUTW(K)=-9999.000
            ELSE
            OUTW(K)=((V80(IX-1,IY-1,1)**2.0)+
     *      (V80(IX-1,IY-1,2)**2.0))**0.5
            END IF
 40         CONTINUE
```

```
 30       CONTINUE
C
C  WRITE TO OUTPUT FILE, WITH GRID DIMENSIONS BEING -2 IN
C  BOTH DIRECTIONS.  CHECK THAT COUNTER (K) EQUALS THE OUTPUT
C  FILE SIZE
C
          IF(K.NE.MDATA) THEN
          PRINT*,'K NOT EQUAL TO MDATA'
          STOP
          ELSE
          END IF
          IR=IR+1
          WRITE(2,REC=IR)(OUTW(NNN),NNN=1,K)
 10    CONTINUE
       STOP
       END
```

APPENDIX 3: Anomalies Identified in the UKMO MSLP Dataset

THE NOVEMBER 1882 LOW PRESSURE ANOMALY

Once the monthly means were created GrADS was used to display an animated contour plot showing every month. Visual examination of the data revealed an unusually high monthly mean (30 ms^{-1}) in November 1882, centred around grid point (10°W, 50°N), south of Ireland. The UKMO daily MSLP data was looked at and an anomaly was identified. The location exhibiting the highest winds had a consistently lower pressure than all surrounding grid points for much of November. This is very unlikely to occur in reality as Atlantic low pressure systems move due to upper atmosphere changes (Ahrens, 1994). The possibility of a low pressure system remaining in this location for a number of weeks is not physically feasible (note: a thermal low may form and remain over a landmass for such a period). To prevent this erroneous result affecting the beginning of the dataset the analysis period was altered to begin in 1883. The loss of two years is not considered detrimental to the overall aims of the project.

THE 18/1/27 HIGH PRESSURE ANOMALY

Examination of the extreme values in the geostrophic winds produced by the model led to the identification of an anomaly in the UKMO pressure dataset. At grid points (0°, 35°N) and (10°E, 35°N), situated above North Africa, the 1200 hr MSLP values are given as 1061 and 1060 hPa respectively for 18/1/27. Values at adjacent grid points are all below 1020 hPa and both the previous and following daily MSLPs show no significant high pressure system. The pressure gradients led to geostrophic wind speeds of over 100 ms^{-1} above the two grid points. There was no discussion of such an intense high in the literature for this time and location. Since the dataset exhibits no spatial or temporal trend supporting the intensification of such high pressures the values were discarded and the daily MSLP grid was replaced with an average of the previous and following day.

APPENDIX 4: The seasonal pattern in wind speeds

The seasonal trend varies significantly over space, figure 16 shows examples of the typical North Atlantic trend (grid point 12) and the trend in the Eastern Mediterranean (grid point 3). There is clearly good agreement between the NCEP/NCAR and derived seasonal trend.

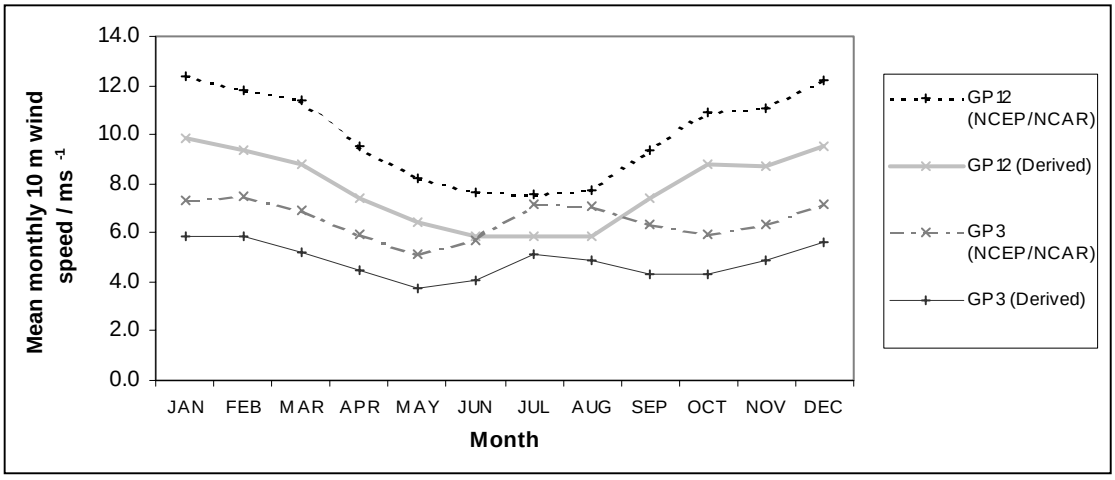

Figure 16. Monthly averages at grid points 3 and 12 in the derived and NCEP/NCAR data.

The Atlantic trend is typical of most grid points showing the highest wind speeds in winter. Grid points 2 and 3 share an unusual summer peak in July and August that is spatially consistent with adjacent grid points. Grid point 2 is located in the Aegean Sea, the climatology of which has been described by Poulos *et al* (1997). The wind field is dominated by northerlies, exhibiting two maxima in the annual trend. The first peak occurs during winter due to strong, cold and dry northerly winds. Then from May to September another northerly associated with clear skies dominates. This summer wind sometimes reaches gale force speeds and persists for long periods during the summer.

Whilst no such climatological feature is identified at grid point 2, comparisons can be made with the measurements at coastal and island locations presented in the EWA (shown in figure 17). Two observation sites near to grid point 2 (Sagres (Portugal) and Fuerteventura (Canary Islands)) experienced highest wind speeds during the July to September period. Both are virtually small islands (Sagres is located on a thin peninsula) so it is unlikely that summer sea-breeze circulations have a strong effect. The geostrophic wind should describe the surface wind adequately. Other sites in Portugal and Spain showed a slight winter maximum but little variation throughout the year. The reason for this localised summer maximum in wind speed has not been explained but may relate to the larger global circulation and the formation of high pressure systems from descending air around 30° N.

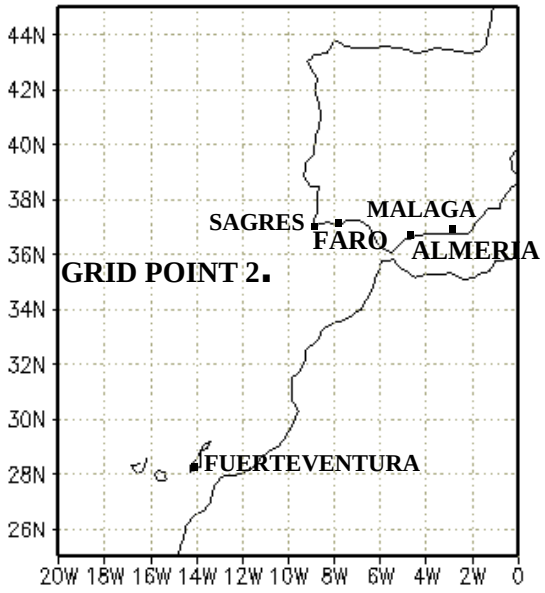

Figure 17. The location of grid point 2 and comparative sites.